



# Evolution of vertebral numbers in primates, with a focus on hominoids and the last common ancestor of hominins and panins

Jeffrey K. Spear<sup>a, b, \*</sup>, Mark Grabowski<sup>c, d</sup>, Yeganeh Sekhavati<sup>e</sup>, Christina E. Costa<sup>a, b</sup>, Deanna M. Goldstein<sup>f</sup>, Lauren A. Petrullo<sup>g</sup>, Amy L. Peterson<sup>h</sup>, Amanda B. Lee<sup>i</sup>, Milena R. Shattuck<sup>j</sup>, Asier Gómez-Olivencia<sup>k, l, m</sup>, Scott A. Williams<sup>a, b</sup>

<sup>a</sup> Center for the Study of Human Origins, Department of Anthropology, New York University, New York, NY, USA

<sup>b</sup> New York Consortium in Evolutionary Primatology, New York, NY, USA

<sup>c</sup> Research Centre in Evolutionary Anthropology and Paleoecology, Liverpool John Moores University, Liverpool, UK

<sup>d</sup> Department of Biosciences, Centre for Ecological and Evolutionary Synthesis, University of Oslo, Oslo, Norway

<sup>e</sup> Department of Anthropology, Washington University in St. Louis, St. Louis, MO, USA

<sup>f</sup> Department of Anatomical Sciences, Renaissance School of Medicine, Stony Brook University, Stony Brook, NY, USA

<sup>g</sup> Department of Psychology, University of Michigan, Ann Arbor, MI, USA

<sup>h</sup> Smithsonian Institution, National Museum of Natural History, Washington DC, USA

<sup>i</sup> Data Scientist, Jellyfish, Suite 3033, 220 N Green St, Chicago, IL, USA

<sup>j</sup> Department of Anthropology, Hunter College CUNY, New York, NY, USA

<sup>k</sup> Departamento de Geología, Facultad de Ciencia y Tecnología, Universidad Del País Vasco/Euskal Herriko Unibertsitatea (UPV/EHU), Barrio Sarriena S/n, 48940 Bilbao, Spain

<sup>l</sup> Sociedad de Ciencias Aranzadi, Zorroagagaina 11, 20014 Donostia-San Sebastián, Spain

<sup>m</sup> Centro UCM-ISCI de Investigación Sobre Evolución y Comportamiento Humanos, Avda. Monforte de Lemos 5 (Pabellón 14), 28029 Madrid, Spain

## ARTICLE INFO

### Article history:

Received 12 October 2022

Accepted 14 March 2023

Available online 24 April 2023

### Keywords:

Vertebral column

Last common ancestor

Hominin evolution

Bipedalism

Ancestral state reconstruction

## ABSTRACT

The primate vertebral column has been extensively studied, with a particular focus on hominoid primates and the last common ancestor of humans and chimpanzees. The number of vertebrae in hominoids—up to and including the last common ancestor of humans and chimpanzees—is subject to considerable debate. However, few formal ancestral state reconstructions exist, and none include a broad sample of primates or account for the correlated evolution of the vertebral column. Here, we conduct an ancestral state reconstruction using a model of evolution that accounts for both homeotic (changes of one type of vertebra to another) and meristic (addition or loss of a vertebra) changes. Our results suggest that ancestral primates were characterized by 29 precaudal vertebrae, with the most common formula being seven cervical, 13 thoracic, six lumbar, and three sacral vertebrae. Extant hominoids evolved tail loss and a reduced lumbar column via sacralization (homeotic transition at the last lumbar vertebra). Our results also indicate that the ancestral hylobatid had seven cervical, 13 thoracic, five lumbar, and four sacral vertebrae, and the ancestral hominid had seven cervical, 13 thoracic, four lumbar, and five sacral vertebrae. The last common ancestor of humans and chimpanzees likely either retained this ancestral hominid formula or was characterized by an additional sacral vertebra, possibly acquired through a homeotic shift at the sacrococcygeal border. Our results support the ‘short-back’ model of hominin vertebral evolution, which postulates that hominins evolved from an ancestor with an African ape—like numerical composition of the vertebral column.

© 2023 Elsevier Ltd. All rights reserved.

## 1. Introduction

The numerical composition of the vertebral column and its evolution have been of interest to natural historians and other

biologists for centuries. Modern understanding of evolutionary processes and the underlying developmental genetics of vertebral segmentation and specification, coupled with increasing phylogenetic resolution, permits research into the conservation and complexity of vertebral numbers among mammals. Numbers of cervical vertebrae are essentially fixed at seven in the vast majority of mammals (Galis, 1999a), and the presacral number (combined cervical, thoracic, and lumbar) is also fairly constrained, at least in

\* Corresponding author.

E-mail address: [jks417@nyu.edu](mailto:jks417@nyu.edu) (J.K. Spear).

certain lineages (Narita and Kuratani, 2005; Galis et al., 2014; Williams et al., 2019b). Mammals that engage in suspensory behavior often depart from and are more variable in presacral numbers of vertebrae than their nonsuspensory close relatives (Williams et al., 2019b). One such group is hominoids (apes and humans), and interpretations of the evolutionary history of both suspensory positional behavior and vertebral numbers in this group are contentious (Latimer and Ward, 1993; Haeusler et al., 2002; Pilbeam, 2004; Rosenman, 2008; Lovejoy et al., 2009; Lovejoy and McCollum, 2010; McCollum et al., 2010; Williams, 2012a; Williams et al., 2016, 2019a; Machnicki et al., 2016; Thompson and Almécija, 2017; Tardieu and Haeusler, 2019; Machnicki and Reno, 2020; Williams and Pilbeam, 2021), in large part due to its implications for the ancestral condition from which hominins evolved bipedal locomotion.

There are currently three models that hypothesize the numbers of vertebrae characterizing the last common ancestor (LCA) of hominins (members of the human lineage) and panins (chimpanzees and bonobos;  $LCA_{H-P}$ ). These focus on the number of lumbar vertebrae, which is the presumed target of selection due to its role in vertical posture and lordosis, the dorsal concavity of the lumbar spine (Lovejoy, 2005; Whitcome et al., 2007; Williams et al., 2022). The 'long-back' model (Fig. 1A) posits that the  $LCA_{H-P}$  maintained six lumbar vertebrae as well as a long thoracic column consisting of 13 elements (Lovejoy et al., 2009; Lovejoy and McCollum, 2010; McCollum et al., 2010; Machnicki and Reno, 2020), together contributing to a 26-element presacral column. The 'intermediate-back' model suggests that the  $LCA_{H-P}$  was characterized by five lumbar vertebrae and either 12 or 13 thoracic vertebrae (Johanson et al., 1982; Haeusler et al., 2002; Machnicki et al., 2016; Tardieu and Haeusler, 2019), totaling either 24 or 25 presacral vertebrae (Fig. 1B). The 'short-back' model posits that the  $LCA_{H-P}$  possessed four lumbar vertebrae and 13 thoracic vertebrae (Pilbeam, 2004; Williams, 2012a; Williams et al., 2016, 2019a; Williams and Pilbeam, 2021), yielding a short presacral column consisting of 24 elements (Fig. 1C).

Among extant taxa, many nonhominoid primates are characterized by a vertebral formula consisting of seven cervical (C), 13 thoracic (T), and six lumbar (L) vertebrae, including many platyrrhine and cercopithecoid monkeys, and this presacral combination was proposed as ancestral for primates, anthropoids, or catarrhines (Schultz and Straus, 1945; Pilbeam, 2004; Williams, 2011, 2012a). Extant African apes, specifically western gorillas (*Gorilla gorilla*) and both chimpanzees (*Pan troglodytes*) and bonobos (*Pan paniscus*), are characterized by 7C, 13T, and 4L modally, while eastern gorillas (*Gorilla beringei*) have one fewer lumbar vertebra (7C, 13T, 3L; Williams et al., 2019a). The latter presacral combination is frequently found in western gorillas, chimpanzees, and bonobos as well (Williams et al., 2019a). Orangutans generally have one fewer thoracic vertebra than chimpanzees, bonobos, and western gorillas (7C, 12T, 4L). Hylobatids (lesser apes or gibbons) are highly variable but most commonly possess 7C, 13T, and 5L. Modern humans are also variable in their vertebral formula, although deviations from the modal formula are less frequent than in most other apes. Humans normally have 7C, 12T, and 5L (Pilbeam, 2004; Williams et al., 2019a).

A variety of approaches have been brought to bear on this question, including parsimony analyses, comparative morphology, and inferences from fossil taxa (Pilbeam, 2004; McCollum et al., 2010; Williams, 2012a; Williams et al., 2019a; Machnicki and Reno, 2020). Two formal ancestral state reconstruction studies have been performed so far (Fulwood and O'Meara, 2014; Thompson and Almécija, 2017). Both studies found the strongest support for the short-back model and the weakest support for the long-back model. Fulwood and O'Meara (2014), however, looked

only at lumbar numbers. Thompson and Almécija (2017) examined all precaudal vertebrae, but each portion of the vertebral column was analyzed independently. This represents a major limitation of their study (which they acknowledge), since conducting the analysis in this way assumes that all changes to different segments of the vertebral column are independent of one another.

Although vertebral formulae (regional numbers of vertebrae) can clearly evolve via meristic change (additions or deletions of vertebrae), which is largely independent in each region of the vertebral column, homeotic changes (regional boundary shifts within the same numerical framework) also appear to be common both inter- and intraspecifically (Galis, 1999b; Wellik and Capecchi, 2003; Williams, 2011; Galis et al., 2014; Williams and Pilbeam, 2021). For example, cercopithecoid monkeys tend to possess either 13T and 6L or 12T and 7L (Schultz and Straus, 1945; Clausier, 1980; Williams, 2011, 2012a), two configurations of 19 thoracic and lumbar vertebrae achievable via homeotic shifts at the thoracolumbar border. Most researchers agree that great apes evolved reduced numbers of lumbar vertebrae via homeotic shifts at the lumbosacral border and that hominoid sacra increased in number due to homeotic shifts at the lumbosacral border or the sacrocaudal border (see Williams and Russo, 2015). Recently, Williams and Pilbeam (2021) proposed that hominins evolved from an  $LCA_{H-P}$  that was specifically paninlike in its full vertebral formula and derived the modal human configuration via a single homeotic shift in Hox10 rostral and caudal expression boundaries.

Homeobox (Hox) gene expression domains are associated with vertebral regional boundaries and are thought to contribute to the development of morphologies typical of different regions (Wellik and Capecchi, 2003; Carapuço et al., 2005; Mallo et al., 2010; Casaca et al., 2014). Shifts in Hox gene expression domains and their effects on vertebral development are therefore homeotic in nature. Since differences among taxa in regional numbers of vertebrae can result from meristic or homeotic change at any regional boundary, ideally full vertebral formulae (cervical, thoracic, lumbar, sacral, caudal/coccygeal) should be used in analyses rather than considering each individual section independently. Here, we use phylogenetic ancestral state reconstruction methods that account for both homeotic and meristic changes on full vertebral formulae of primates to understand how vertebral numbers evolved and test hypotheses regarding the number of vertebrae in ancestral apes.

## 2. Materials and methods

### 2.1. Samples

Data were collected at natural history museums and university collections around the world (Supplementary Online Material [SOM] Table S1). Specimens were articulated to check for completeness, and numbers of cervical, thoracic, lumbar, and caudal (or coccygeal in the case of animals lacking an external tail) vertebrae were recorded. The number of elements composing the sacrum and the number of coccygeal segments (if relevant) were recorded. Taxa were included in the analysis if they were represented by at least four individuals in the data set. The Schultz (1961) definition of thoracic and lumbar vertebrae based on rib presence (thoracic) or absence (lumbar) was used (also see Schultz and Straus, 1945; Williams and Pilbeam, 2021). For the purposes of this study, individuals with incomplete homeotic transitions (e.g., 12.5 thoracic and 4.5 lumbar) were treated as half a count for each whole number vertebral formula (e.g., 0.5 for 13 thoracic/4 lumbar and 0.5 for 12 thoracic/5 lumbar) rather than individuals with unique formulae. The total sample includes 6216 individuals representing 141 species (Table 1).

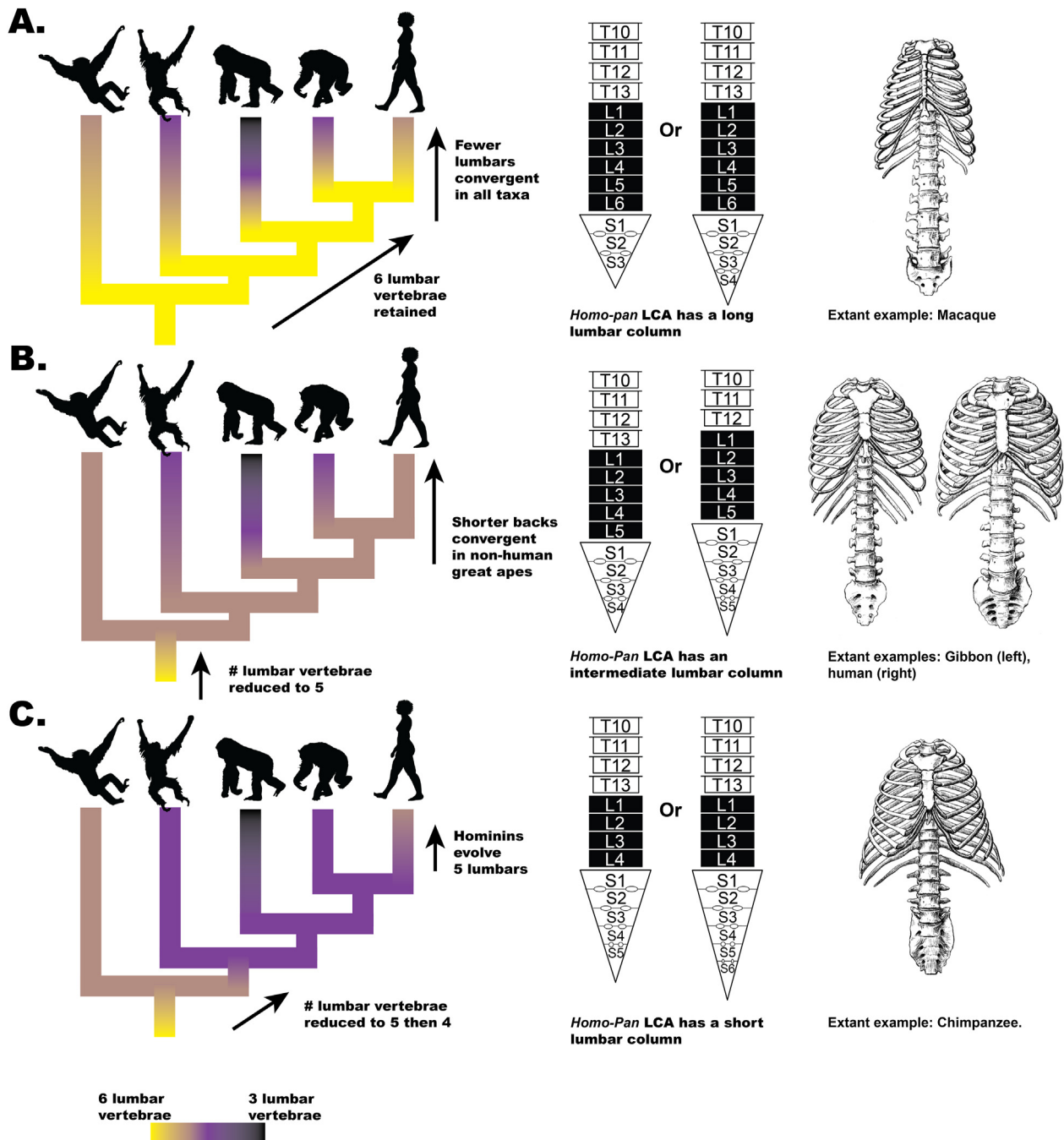


**Figure 1.** Visual representations of the different models for the last common ancestor of hominins and panins. A) Long-back model, with 13 thoracic vertebrae, six lumbar vertebrae, and four sacral vertebrae. B) Intermediate-back models, one with 13 thoracic vertebrae, five lumbar vertebrae, and four sacral vertebrae and the other with 12 thoracic vertebrae, five lumbar vertebrae, and five sacral vertebrae. C) Short-back model, with 13 thoracic vertebrae, four lumbar vertebrae, and five sacral vertebrae. Illustrations modified from Schultz (1950). Silhouettes from PhyloPic.org.

## 2.2. Phylogeny

For this analysis, we used the recent mammal phylogeny published by Upham et al. (2019). This phylogeny strongly samples both primate and nonprimate taxa and is better resolved than earlier mammal phylogenies (e.g., Bininda-Emonds et al., 2007). We could not use an order-wide primate phylogeny as those in common use (e.g., Arnold et al., 2010; Springer et al., 2012) do not include sufficient outgroups for the primate-wide analysis.

## 2.3. Data analysis

We performed two ancestral character state reconstructions. Due to computational limitations, we were unable to include variation in all types of vertebrae across all primates. Therefore, we limited our analysis of the entire primate order (and relevant outgroups) to precaudal vertebrae. For our analysis that included caudal vertebrae, we focused on apes specifically, which allowed us to use fewer taxa and character states, and thus make the analysis computationally feasible.

**Table 1**

Taxa and specimens.

Order Family Genus and species	Analyses used	Number of individuals	Number of polymorphisms	
			Analysis 1	Analysis 2 <sup>a</sup>
Rodentia				
Muridae				
<i>Rattus norvegicus</i>	1	45	2	N/A
Dipodidae				
<i>Jaculus orientalis</i>	1	19	1	N/A
Castoridae				
<i>Castor canadensis</i>	1	54	1	N/A
Heteromyidae				
<i>Dipodomys ordii</i>	1	17	2	N/A
Pedetidae				
<i>Pedetes capensis</i>	1	21	1	N/A
Sciuridae				
<i>Tamiasciurus hudsonicus</i>	1	20	2	N/A
Apododontidae				
<i>Apodontia rufa</i>	1	17	1	N/A
Chinchillidae				
<i>Lagostomus maximus</i>	1	11	1	N/A
Echimyidae				
<i>Myocastor coypus</i>	1	23	3	N/A
Lagomorpha				
Leporidae				
<i>Lepus timidus</i>	1	14	2	N/A
Dermoptera				
Cynocephalidae				
<i>Cynocephalus volans</i>	1	16	3	N/A
<i>Galeopterus variegatus</i>	1	17	4	N/A
Scandentia				
Tupaiaidae				
<i>Tupaia glis</i>	1	8	1	N/A
<i>Tupaia minor</i>	1	4	2	N/A
Ptilocercidae				
<i>Ptilocercus lowii</i>	1	8	3	N/A
Primates				
Lorisidae				
<i>Perodicticus potto</i>	1	45	3	N/A
<i>Arctocebus calabarensis</i>	1	25	5	N/A
<i>Nycticebus coucang</i>	1	29	2	N/A
<i>Loris tardigradus</i>	1	19	3	N/A
<i>Loris lydekkerianus</i>	1	6	3	N/A
Galagidae				
<i>Galagoides demidovii</i>	1	12	3	N/A
<i>Otolemur garnettii</i>	1	12	2	N/A
<i>Otolemur crassicaudatus</i>	1	21	1	N/A
<i>Galago moholi</i>	1	5	1	N/A
<i>Galago gallarum</i>	1	6	3	N/A
<i>Galago senegalensis</i>	1	15	1	N/A
<i>Euoticus elegantulus</i>	1	53	3	N/A
Daubentonidae				
<i>Daubentonia madagascariensis</i>	1	9	2	N/A
Lemuridae				
<i>Varecia variegata</i>	1	12	1	N/A
<i>Lemur catta</i>	1	14	4	N/A
<i>Hapalemur griseus</i>	1	9	1	N/A
<i>Eulemur mongoz</i>	1	13	2	N/A
<i>Eulemur coronatus</i>	1	4	2	N/A
<i>Eulemur collaris</i>	1	9	2	N/A
<i>Eulemur fulvus</i>	1	12	1	N/A
<i>Eulemur albifrons</i>	1	16	1	N/A
<i>Eulemur rufus</i>	1	6	2	N/A
<i>Eulemur macaco</i>	1	13	2	N/A
Cheirogaelidae				
<i>Cheirogaleus major</i>	1	7	4	N/A
<i>Cheirogaleus medius</i>	1	5	2	N/A
<i>Microcebus murinus</i>	1	9	4	N/A
Lepilemuridae				
<i>Lepilemur ruficaudatus</i>	1	13	1	N/A
Indriidae				
<i>Propithecus diadema</i>	1	9	1	N/A
<i>Propithecus verreauxi</i>	1	10	5	N/A
<i>Avahi laniger</i>	1	12	1	N/A
<i>Indri indri</i>	1	27	3	N/A

Table 1 (continued)

Order	Analyses used	Number of individuals	Number of polymorphisms	
			Analysis 1	Analysis 2 <sup>a</sup>
Family				
Genus and species				
<i>Phaner furcifer</i>	1	4	1	N/A
Tarsidae				
<i>Tarsius bancanus</i>	1 and 2	6	1	1
<i>Tarsius tarsier</i>	1	4	1	N/A
Aotidae				
<i>Aotus trivirgatus</i>	1	4	2	N/A
<i>Aotus azarae</i>	1	34	1	N/A
Callitrichidae				
<i>Saguinus midas</i>	1	5	3	N/A
<i>Saguinus oedipus</i>	1 and 2	20	2	2
<i>Leontopithecus rosalia</i>	1	8	3	N/A
<i>Callithrix jacchus</i>	1 and 2	22	1	1
<i>Callimico goeldii</i>	1	8	3	N/A
Cebidae				
<i>Saimiri sciureus</i>	1 and 2	53	2	2
<i>Sapajus apella</i>	1 and 2	38	4	4
<i>Cebus albifrons</i>	1	29	3	N/A
<i>Cebus capucinus</i>	1 and 2	29	3	3
Atelidae				
<i>Lagothrix lagotricha</i>	1 and 2	36	2	2
<i>Lagothrix cana</i>	1	9	6	N/A
<i>Brachyteles arachnoides</i>	1	10	4	N/A
<i>Ateles paniscus</i>	1	16	1	N/A
<i>Ateles belzebuth</i>	1	10	1	N/A
<i>Ateles geoffroyi</i>	1 and 2	16	1	1
<i>Ateles fusciceps</i>	1	7	4	N/A
<i>Alouatta pigra</i>	1	4	2	N/A
<i>Alouatta palliata</i>	1	14	2	N/A
<i>Alouatta caraya</i>	1	4	3	N/A
<i>Alouatta seniculus</i>	1 and 2	25	2	2
Pitheciidae				
<i>Callicebus moloch</i>	1	6	4	N/A
<i>Pithecia pithecia</i>	1	13	3	N/A
<i>Pithecia monachus</i>	1	4	2	N/A
<i>Cacajao calvus</i>	1	5	3	N/A
<i>Cacajao melanocephalus</i>	1	8	3	N/A
Hylobatidae				
<i>Nomascus leucogenys</i>	1 and 2	4	4	16*
<i>Nomascus gabriellae</i>	1 and 2	14	2	8*
<i>Nomascus concolor</i>	1 and 2	25	2	1
<i>Hylobates pileatus</i>	1 and 2	7	3	12*
<i>Hylobates lar</i>	1 and 2	266	2	4
<i>Hylobates muelleri</i>	1 and 2	35	2	6*
<i>Hylobates klossii</i>	1 and 2	12	3	12*
<i>Hylobates moloch</i>	1 and 2	38	2	6*
<i>Hylobates agilis</i>	1 and 2	37	2	8*
<i>Symphalangus syndactylus</i>	1 and 2	98	3	6
<i>Hoolock hoolock</i>	1 and 2	34	2	3
Hominidae				
<i>Pongo pygmaeus</i>	1 and 2	142	2	4
<i>Pongo abelii</i>	1 and 2	48	3	4
<i>Pan troglodytes</i>	1 and 2	525	4	8
<i>Pan paniscus</i>	1 and 2	55	2	3
<i>Homo sapiens</i>	1 and 2	893	2	3
<i>Gorilla gorilla</i>	1 and 2	409	4	5
<i>Gorilla beringei</i>	1 and 2	109	2	2
Cercopithecidae				
<i>Trachypithecus phayrei</i>	1	23	1	N/A
<i>Trachypithecus obscurus</i>	1	23	2	N/A
<i>Trachypithecus cristatus</i>	1 and 2	118	1	1
<i>Trachypithecus vetulus</i>	1	4	2	N/A
<i>Semnopithecus entellus</i>	1 and 2	18	2	2
<i>Presbytis melalophos</i>	1	19	2	N/A
<i>Presbytis rubicunda</i>	1	5	2	N/A
<i>Pygathrix nemaeus</i>	1	7	1	N/A
<i>Nasalis larvatus</i>	1 and 2	59	1	1
<i>Procolobus verus</i>	1	4	2	N/A
<i>Procolobus badius</i>	1	40	3	N/A
<i>Colobus guereza</i>	1	44	1	N/A
<i>Colobus angolensis</i>	1	9	1	N/A
<i>Macaca sylvanus</i>	1	22	1	N/A

(continued on next page)



Table 1 (continued)

Order	Analyses used	Number of individuals	Number of polymorphisms	
			Analysis 1	Analysis 2 <sup>a</sup>
Family				
Genus and species				
<i>Macaca nemestrina</i>	1	15	2	N/A
<i>Macaca fascicularis</i>	1 and 2	98	2	1
<i>Macaca fuscata</i>	1	884	1	N/A
<i>Macaca mulatta</i>	1	42	2	N/A
<i>Macaca arctoides</i>	1 and 2	29	2	2
<i>Theropithecus gelada</i>	1	32	1	N/A
<i>Papio papio</i>	1	17	3	N/A
<i>Papio hamadryas</i>	1	35	1	N/A
<i>Papio anubis</i>	1 and 2	59	2	2
<i>Papio cynocephalus</i>	1	62	2	N/A
<i>Papio ursinus</i>	1	13	1	N/A
<i>Lophocebus aterrimus</i>	1	21	2	N/A
<i>Mandrillus sphinx</i>	1	31	4	N/A
<i>Mandrillus leucophaeus</i>	1 and 2	20	3	3
<i>Lophocebus albigena</i>	1 and 2	87	1	1
<i>Cercocebus torquatus</i>	1	16	1	N/A
<i>Cercocebus atys</i>	1	13	2	N/A
<i>Cercocebus chrysogaster</i>	1	14	2	N/A
<i>Cercocebus agilis</i>	1	10	2	N/A
<i>Cercopithecus neglectus</i>	1	16	2	N/A
<i>Cercopithecus pogonias</i>	1	24	2	N/A
<i>Cercopithecus mona</i>	1	13	3	N/A
<i>Cercopithecus nictitans</i>	1	22	3	N/A
<i>Cercopithecus mitis</i>	1	28	2	N/A
<i>Cercopithecus ascanius</i>	1	117	3	N/A
<i>Cercopithecus cephus</i>	1	35	2	N/A
<i>Cercopithecus lhoesti</i>	1	9	1	N/A
<i>Erythrocebus patas</i>	1 and 2	35	1	1
<i>Chlorocebus cynosuros</i>	1	10	1	N/A
<i>Chlorocebus aethiops</i>	1	17	3	N/A
<i>Chlorocebus pygerythrus</i>	1	13	2	N/A
<i>Chlorocebus sabaeus</i>	1	15	1	N/A
<i>Miopithecus talapoin</i>	1 and 2	16	2	2
Total		6216		

N/A = not applicable (i.e., taxon was not used in analysis 2).

<sup>a</sup> Star (\*) indicates that a uniform prior was included for the caudal count associated with at least one cervical-thoracic-lumbar-sacral formula.

We performed ancestral state reconstructions using the `make.simmap` and `describe.simmap` functions in the `phytools` package (Revell, 2012) in the R statistical environment using R v. 4.1.1 (R Core Team, 2022). The `make.simmap` function implements the stochastic character mapping method of Bollback (2006), and `describe.simmap` summarizes the posterior distributions of all simulations. The SIMMAP method simulates character state transition across the tree under an instantaneous transition rate, or  $M_{ik}$  model (Lewis, 2001). Rates of transitions between different character states are represented using an instantaneous rate matrix (Q matrix). The SIMMAP method can accommodate uncertainties in tip states. These simulations can be run multiple times, and a posterior distribution of states is generated for each node and tip. For each reconstruction, we generated 5000 character histories. Posterior probabilities for ancestral states at each node represent the frequency that each state appears at that node across those 5000 stochastic simulations. Once the simulations were run, we examined both the posterior probability of different character states at relevant nodes in the primate tree as well as the 95% highest posterior density (HPD) intervals for each vertebral type at each node. The HPD interval represents the range of values that includes 95% of the posterior distribution, centered on the value with the highest posterior probability. Highest posterior density intervals were calculated using the `HPDinterval` function in the `coda` package in R (Plummer et al., 2006).

In the first reconstruction (analysis 1), we examined the pre-caudal vertebral numbers across Primates. To allow us to estimate ancestral conditions near the base of the primate tree, we also

included data from the four orders most closely related to Primates: Dermoptera, Scandentia, Lagomorpha, and Rodentia. Outgroup taxa were chosen to be representative of the diversity of different vertebral formulae in these groups. Dermoptera is represented by two extant genera, Scandentia is represented by six species representing both extant families, Lagomorpha is represented by a single species (*Lepus timidus*), and Rodentia is represented by nine species from nine families (see Table 1). Ideally, our sample would have included pikas within Lagomorpha. We encountered very few specimens during data collection, however, and Tague's (2017) large samples of lagomorphs cannot be compiled with our data due to differences in data collection (i.e., Tague, 2017 did not follow the Schultz criteria in recording 'half counts' for asymmetrical, 'intermediate' vertebrae).

Possible character states for each section of the column include cervical (7), thoracic (12 or fewer, 13, 14, 15 or more), lumbar (3, 4, 5, 6, 7, 8 or more), and sacral (2, 3, 4, 5, 6, 7). Collectively, these make 144 unique character states. Prior probabilities were applied to each tip based on the frequency that a given condition is observed in a given taxon in our data set. All absolute frequencies over 10% were included. In addition, we ran a broken stick model (MacArthur, 1957) to determine whether any variants represented at below 10% frequency should also be included. Variants were included if they were represented in more than 10% of individuals or were represented in fewer than 10% of individuals but in more individuals than would be expected under a random distribution. None of the character states eliminated during binning (e.g., 11 thoracic vertebrae binned with 12) represented a majority or plurality of any taxon studied.

The Q matrix (the instantaneous rate matrix for the  $M_k$  model) is calculated using maximum likelihood, contingent on tip states, and a specified rate heterogeneity. The default rate heterogeneity in the make.simmap function is a symmetrical model in which transitions between each pair of character states occur at the same rate in both directions, but transitions between different pairs occur at different rates. For example, the rate of a transition between 7C–12T–7L–3S  $\rightarrow$  7C–13T–6L–3S is the same as 7C–13T–6L–3S  $\rightarrow$  7C–12T–7L–3S, but 7C–12T–7L–3S  $\leftrightarrow$  7C–12T–7L–4S is different. Using this default model in our analyses, however, would involve 10,000 unique rate parameters, which is unfeasible. An alternative model is an equal rates model, in which transitions among all character states occur at the same rate. This model involves only a single rate parameter, but it means, for example, that a change between 7C–12T–7L–3S  $\leftrightarrow$  7C–13T–6L–3S (a single homeotic shift) occurs at the same rate as a change from 7C–12T–7L–3S  $\leftrightarrow$  7C–14T–3L–6S (multiple homeotic and meristic shifts), which is incompatible with current research on vertebral development.

In light of these issues with the default models, we used a custom model that accounts for prior understanding of how numbers of vertebrae evolve while also minimizing the number of parameters in the model. Our model (SOM Table S2) included only two types of character transitions: the addition or removal of one vertebra (representing a meristic change) and a vertebra changing from one type into a neighboring type (representing a homeotic change). The rates of homeotic and meristic changes are independent of one another, but the model assumes that all homeotic transitions happen at the same rate, and all meristic transitions happen at the same rate. All other types of transitions were set to a rate of 0. This means that it is not possible for a lineage to gain or lose two vertebrae at the same time, but since the  $M_k$  model treats transitions as instantaneous, independent, and reversible, it is possible for two transitions to occur along the same branch of the tree, leading to multiple changes between adjacent nodes (made more likely the longer the branch is).

In the second reconstruction (analysis 2), we examined the full vertebral column numbers, including caudal/coccygeal vertebrae, in apes. As outgroups for apes, we included a representative sampling of cercopithecoids and platyrrhines, as well as a tarsier. By limiting the analysis in this way we could use fewer taxa and possible character states and therefore make the analysis that included caudal vertebrae computationally feasible. Possible character states for each section of the column include cervical (7); thoracic (12, 13, 14 or more); lumbar (3, 4, 5, 6, 7 or more); sacral (3, 4, 5, 6); and caudal (2, 3, 4, 5, 6 or more). Together, these make a total of 300 character states. To reduce this number and improve computation time, we first ran 100 simulations and examined which areas of morphospace were utilized in those simulations. We found that no lineage in any of these 100 simulations ever passed through a condition of having 12 thoracic vertebrae and 3 lumbar vertebrae or 14 thoracic vertebrae and 7 lumbar vertebrae. Therefore, we eliminated these possibilities to improve computation time, leaving 260 possible character states. As with the first analysis, prior probabilities were applied to each tip based on the frequency that a given condition is observed in a given taxon in our data set. All absolute frequencies over 10% were included, and a broken stick model was used to determine whether additional variants with absolute frequencies below 10% should be included. Several hylobatid species lacked four individuals with caudal counts. These taxa were included using a uniform prior for each possible caudal length except 6+ (presence of an external tail). Except for variation in tail length, which is condensed into the single state of 6+ caudal vertebrae (i.e., possessing a tail), none of the character states eliminated during binning (e.g., 15 thoracic

vertebrae binned with 14) represented a majority or plurality of any taxon studied.

As with analysis 1, practical and theoretical concerns precluded the use of default models for the rate heterogeneity of the Q matrix and we therefore used a custom model (SOM Table S3). In analysis 2, we set three unique rates for the Q matrix: the addition or removal of one vertebra (representing a meristic change); a vertebra changing from one type into a neighboring type (representing a homeotic change); and any changes between 5 and 6+ caudal vertebrae. Because of the large amount of variation binned in the 6+ state, it would be inappropriate to treat a transition from 5 to 6+ caudal vertebrae as identical to a transition from 5 to 4 caudal vertebrae. As in analysis 1, other types of transitions were set to a rate of 0.

### 3. Results

#### 3.1. Analysis 1

Posterior probabilities for all vertebral formulae in analysis 1 are given in SOM Table S4, and 95% HPDs are given in SOM Table S5. A summary of results is given in Table 2. Additional summaries of results showing only different thoracic (SOM Table S6; SOM Fig. S1), lumbar (SOM Table S7; SOM Fig. S2), sacral (SOM Table S8; SOM Fig. S3), precaudal (SOM Table S9; SOM Fig. S4), and presacral (SOM Table S10; SOM Fig. S5) counts are given in the SOM. Node labels used in SOM Tables S4–S10 are shown in the tree in SOM Figure S6.

Analysis 1 shows that vertebral numbers are fairly conserved in primates, especially within major primate clades: Anthropoidea, Platyrrhini, and Catarrhini are all reconstructed, with strong support, as having 29 precaudal vertebrae (>95% posterior probability for all three clades, 95% HPD includes only 29 presacral vertebrae) and 26 presacral vertebrae (>88% for all three clades, 95% HPD is 26–25 for anthropoids and catarrhines and 26 only for platyrrhines). The single formula with the highest posterior probability is 7C–13T–6L–3S (anthropoids 80%; catarrhines 69%; platyrrhines 95%). Twenty-six presacral vertebrae are also the condition recovered for the LCA of haplorhines (87%; 95% HPD 26–27) and primates as a whole (86% 95% HPD 26–27). Twenty-nine precaudal vertebrae are also most common at these nodes, but support is more tentative (65% for haplorhines, 95% HPD 29–30; 54% for primates, 95% HPD 29–31), with 30 precaudal vertebrae being the most probable alternative (35% for haplorhines, 45% for primates). Ancestral primates probably had 13 thoracic vertebrae (79%; 12 thoracic vertebrae 20%; 95% HPD 12–13), six lumbar vertebrae (67%; 95% HPD six to seven), and three sacral vertebrae (67%; 95% HPD three to four). In haplorhines, the specific formulae with the highest posterior probabilities are 7C–13T–6L–3S (48%), 7C–13T–6L–4S (22%), and 7C–12T–7L–3S (15%). In primates, the most commonly recovered ancestral condition is 7C–13T–6L–3S (38%), although 7C–13T–6L–4S (28%) and 7C–12T–7L–3S (15%) are also common. An overview of primate vertebral evolution, showing the formulae with the highest posterior probabilities, is given in Figure 2.

Nearly all haplorhine subgroups down to the family level (except Aotidae) retain the ancestral haplorhine condition of 29 precaudal vertebrae (Platyrrhini, Pitheciidae, Callitrichidae, Catarrhini, Cercopithecidae, Hominoidea, Hylobatidae, Tarsiidae all >95% posterior probability and 95% HPD 29 only; Atelidae 92% posterior probability, 95% HPD 28–29; Hominidae 95% HPD 28–29; Cebidae 74% posterior probability, 95% HPD 29–30). The ancestral haplorhine condition of 26 presacral vertebrae is also retained in the ancestors of most major haplorhine clades (Platyrrhini, Pitheciidae, Callitrichidae, Cercopithecidae, Tarsiidae all >95%, 95% HPD 26 only; Atelidae 92%, 95% HPD 25–26; Cebidae 74%, 95% HPD 26–27;

**Table 2**

Summary of selected results of analysis 1, including full formula and lumbar counts.

Node	Full formulae >5%	Posterior probability (full formula)	Lumbar counts >5%	Posterior probability (lumbar count)	95% highest posterior density for lumbar count
Primates	7C 13T 6L 3S	38.4%	6	67.3%	6–7
	7C 13T 6L 4S	28.3%	7	31.7%	
	7C 12T 7L 3S	15.3%			
Strepsirrhines	7C 13T 7L 3S	12.1%			6–8
	7C 13T 7L 3S	38.8%	7	58.8%	
	7C 13T 6L 4S	16.2%	6	34.0%	
	7C 13T 6L 3S	12.9%	8	6.8%	
Lorisids	7C 12T 7L 3S	8.3%			6–7
	7C 14T 7L 4S	35.4%	7	78.8%	
	7C 15T 7L 4S	16.7%	6	17.6%	
	7C 14T 7L 5S	7.2%			
Galagids	7C 14T 7L 3S	6.2%			6
	7C 14T 6L 4S	6.0%			
	7C 13T 6L 3S	76.8%	6	95.9%	
Lemuroids	7C 14T 6L 3S	15.9%			6–8
	7C 13T 7L 3S	45.1%	7	64.2%	
	7C 12T 7L 3S	13.0%	6	22.2%	
	7C 12T 8L 3S	11.9%	8	13.4%	
Indriids	7C 13T 6L 3S	11.9%			8
	7C 13T 6L 4S	8.1%			
	7C 12T 8L 3S	99.2%	8	99.2%	
	7C 13T 6L 3S	47.6%	6	70.7%	
Haplorhines	7C 13T 6L 4S	22.0%	7	27.7%	6–7
	7C 12T 7L 3S	15.0%			
	7C 13T 7L 3S	10.0%			
Anthropoids	7C 13T 6L 3S	79.9%	6	83.5%	6–7
	7C 12T 7L 3S	11.9%	7	13.4%	
Platyrrhines	7C 13T 6L 3S	94.5%	6	94.7%	6–7
			7	5.2%	
			5	92.5%	
Atelids	7C 14T 5L 3S	88.8%	5	95.6%	4–5
Atelines	7C 14T 4L 3S	94.7%	4	95.6%	4
Catarrhines	7C 13T 6L 3S	69.2%	6	74.1%	5–7
	7C 12T 7L 3S	17.7%	7	18.2%	
	7C 13T 5L 4S	7.4%	5	7.7%	
Cercopithecoids	7C 12T 7L 3S	99.1%	7	99.1%	7
Hominoids	7C 13T 5L 4S	88.8%	5	92.0%	4–5
Hylobatids	7C 13T 5L 4S	97.4%	5	>99.9%	5
Hominids	7C 13T 4L 5S	85.7%	4	92.0%	4–5
Hominines			5	6.4%	3–4
	7C 13T 4L 5S	69.5%	4	89.9%	
	7C 13T 4L 6S	18.4%	3	9.1%	
<i>Pongo</i>	7C 13T 3L 6S	9.0%			4
	7C 12T 4L 5S	94.0%	4	>99.9%	
<i>Gorilla</i>	7C 12T 4L 6S	5.9%			3–4
	7C 13T 3L 6S	85.9%	3	86.0%	
<i>Pan-Homo</i>	7C 13T 4L 5S	11.2%	4	14.0%	4
	7C 13T 4L 5S	59.3%	4	96.8%	
<i>Pan</i>	7C 13T 4L 6S	39.4%			4
	7C 13T 4L 6S	77.2%	4	99.6%	
	7C 13T 4L 5S	22.3%			

Abbreviations: C = cervical vertebrae; T = thoracic vertebrae; L = lumbar vertebrae; S = sacral vertebrae.

Catarrhini 88% 95% HPD 25–26). We recovered strong support for an ancestral condition of 7C–13T–6L–3S for platyrrhines (95%) and one of its families, Pitheciidae (93%), and more tentative support among other platyrrhine families (Callitrichidae: 66%, Cebidae: 72%). We also found tentative support for this formula being the ancestral condition of all catarrhines (68%). We recovered strong evidence for homeotic shifts in thoracic and lumbar counts at the base of families Cercopithecidae and Atelidae. Cercopithecids evolved a longer lower back with extremely strong support for an ancestral condition of 7C–12T–7L–3S (99%). Atelids evolved a shorter lumbar column; the most commonly recovered condition was 7C–14T–5L–3S (89%).

We recovered strong support for a reduced presacral count of 25 presacral vertebrae in ancestors of both hominoids (93%, 95% HPD 24–25) and atelines (96%; 95% HPD includes only 25). Twenty-five presacral vertebrae were retained in hylobatids (>99%), but a

further reduction in the presacral count to 24 was recovered for hominids (91%; 95% HPD 23–24). The single formula for the ancestor of atelines with the highest posterior probability is 7C–14T–4L–3S (95%). In atelines, reduction to four lumbar vertebrae was accomplished by a meristic change as there is no concomitant increase in sacral numbers, in contrast with hominoids. In hominoids and hominids, the reduction in presacral vertebrae was accomplished through homeotic transitions, and there is a concomitant reduction in lumbar vertebrae and an increase in the number of sacral vertebrae. The most common single formula recovered as ancestral for hominoids is 7C–13T–5L–4S (89%) and the most common single formula recovered as ancestral for hominids is 7C–13T–4L–5S (86%).

We recovered evidence for several additional shifts within Hominidae. *Pongo* underwent a meristic shift, losing a single thoracic vertebra to 7C–12T–4L–5S (94%). The LCA of Homininae



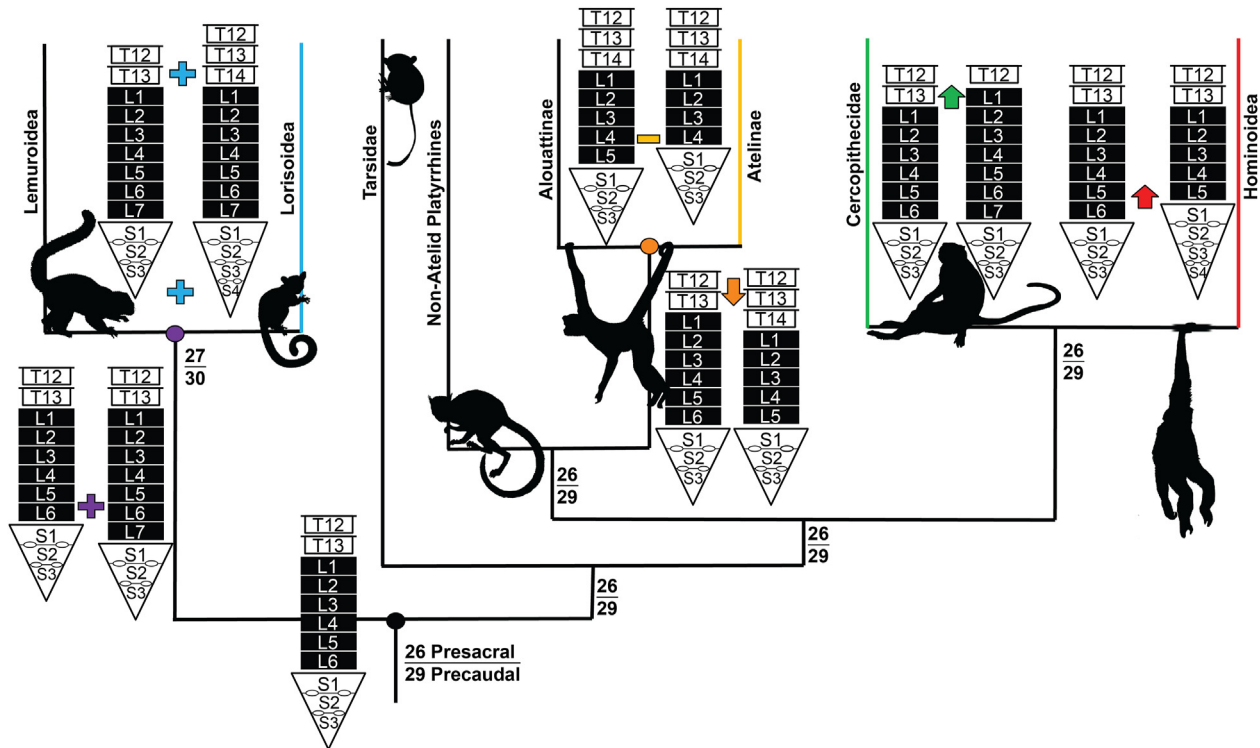


**Figure 2.** Summary of results with highest posterior probabilities for major clades of primates (Order Primates). The lower thoracic column, lumbar column, and sacrum are diagrammed ancestrally and on each stem. Transitions are shown (plus symbol = meristic addition of an element; minus symbol = meristic loss of an element; downward facing arrow = caudally directed homeotic shift; upward facing arrow = cranially directed homeotic shift), and colors correspond to nodes and lineages (e.g., purple = strepsirrhine node). Combined numbers of presacral (C + T + L) and precaudal (C + T + L + S) are listed at nodes. Silhouettes from [PhyloPic.org](https://www.phylopic.org/). (For interpretation of the references to color in this figure legend, the reader is referred to the Web version of this article.)

retained the ancestral hominid formula of 7C–13T–4L–5S (70%; the next most common is 7C–13T–4L–6S, at 18%). The LCA of chimpanzees and humans also likely retained this vertebral formula (59%), although an increase in the number of sacral vertebrae to 7C–13T–4L–6S also receives some support (35%). The LCA of both species of *Pan* either evolved or retained this latter formula (77%). *Gorilla* underwent a homeotic shift reducing the number of lumbar vertebrae and increasing the number of sacral vertebrae to 7C–13T–3L–6S (86%). An overview of hominid vertebral evolution showing the formulae with the highest posterior probabilities is given in [Figure 3](#).

The ancestral strepsirrhine is tentatively recovered as having 30 precaudal vertebrae (68% posterior probability), an increase in one from the ancestral primate, although 29 precaudal vertebrae (22%) also represent a substantial minority (95% HPD 29–31). The number of presacral vertebrae in the ancestral strepsirrhine is recovered as being either 26 (43%) or 27 (54%) (95% HPD 26–27). The most probable single formula is 7C–13T–7L–3S (39%). The only other formulae above 10% posterior probability are the possible ancestral primate formulae, 7C–13T–6L–4S (16%) and 7C–13T–6L–3S (13%). This pattern was retained in ancestral lemuroids (30 precaudal: 71%; 29 precaudal 26%; 95% HPD 29–30; 27 presacral: 61%; 26 presacral: 37%; 95% HPD 26–27; most common single formula: 7C–13T–7L–3S, 45%; 7C–12T–7L–3S, 7C–12T–8L–3S, and 7C–13T–6L–3S are all between 11 and 14%). Indriids further increase the number of lumbar vertebrae to eight through a homeotic transition at the thoracolumbar border, with the most common formula being 7C–12T–8L–3S (99%).

We recovered substantial changes at the base of Lorisiformes. Lorisiformes are found to evolve an additional sacral (four sacral, 70%; five sacral, 17%; 95% HPD three to five) and at least one

additional presacral vertebra (28 presacral: 56%), possibly two (29 presacral: 26%; 95% HPD 27–29). These additional presacral vertebrae were likely thoracic vertebrae (14 thoracic: 60%; 15 thoracic: 32%; 95% HPD 13–15 thoracic), and the most common ancestral loroid formulae are 7C–14T–7L–4S (35%) and 7C–15T–7L–4S (17%). No others are above 8%. Galagids are found to have reduced the number of vertebrae, with 13 thoracic vertebrae (82%; 95% HPD 13–14), six lumbar vertebrae (96%), and three sacral vertebrae (97%). The most common single formula is the most probable ancestral primate formula, 7C–13T–6L–3S (76%; 7C–14T–6L–3S has the next highest posterior probability at 16%).

### 3.2. Analysis 2

Posterior probabilities for all vertebral formulae in analysis 2 are given in [SOM Table S11](#), and 95% HPDs are given in [SOM Table S12](#). A summary of results is given in [Table 3](#). Additional summaries of results showing only different thoracic ([SOM Table S13](#); [SOM Fig. S7](#)), lumbar ([SOM Table S14](#); [SOM Fig. S8](#)), sacral ([SOM Table S15](#); [SOM Fig. S9](#)), caudal/coccygeal ([SOM Table S16](#); [SOM Fig. S10](#)), precaudal ([SOM Table S17](#); [SOM Fig. S11](#)), and presacral ([SOM Table S18](#); [SOM Fig. S12](#)) counts are given in the SOM. Node labels used in [SOM Tables S11–S18](#) are shown in the tree in [SOM Figure S13](#).

In analysis 2, with its more limited taxonomic scope, the resolution of clades above the superfamily level is poor. The ancestral catarrhine pattern with the highest posterior probability is 26 presacral vertebrae (57%), 29 precaudal vertebrae (67%), and an external tail (94%). Twenty-five presacral (38%) and 28 precaudal (27%) also have notable posterior probabilities. Ninety-five percent HPD is 25–26 presacral and 27–29 precaudal. The most probable

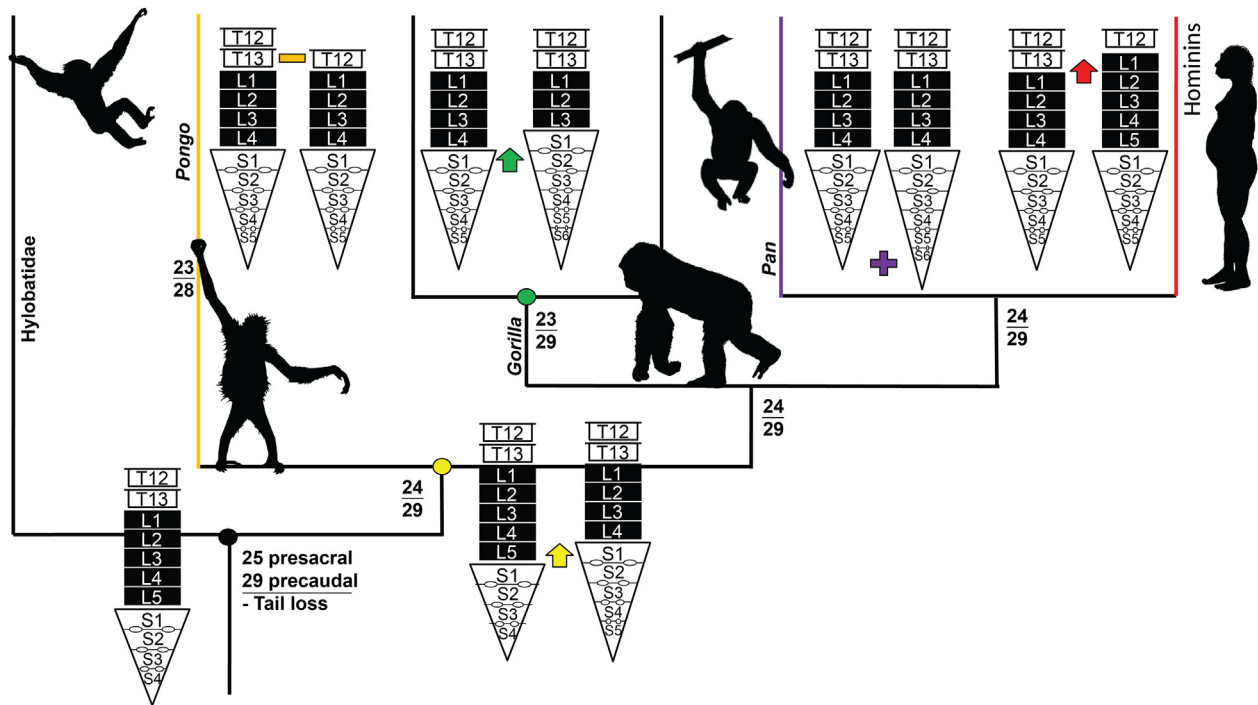


**Figure 3.** Summary of results with highest posterior probabilities in hominoids (Family Hominoidea). Vertebra diagrams and symbols are the same as in Figure 2. Note that this figure supported the results of analysis 1. Analysis 2 supports an LCA<sub>H+P</sub> with six sacral vertebrae and 30 precaudal vertebrae, but is otherwise the same. Silhouettes from [PhyloPic.org](https://www.phylopic.org).

single formulae are 7C–13T–6L–3S–6+Ca (27%) and 7C–12T–7L–3S–6+Ca (23%).

The common ancestor of hominoids likely underwent a shift to a lower presacral count (25 presacral vertebrae: 69%; 24 presacral vertebrae: 27%; 95% HPD 24–25). The precise vertebral formula at the base of Hominoidea is poorly resolved, but this reduction in presacral vertebrae is very likely driven by a reduced number of lumbar vertebrae (five lumbar vertebrae: 69%; four lumbar vertebrae: 19%; 95% HPD four to six). The most common formula is 7C–13T–5L–4S–3Ca (19%), and only four individual formulae are above 5% posterior probability (7C–13T–5L–4S–4Ca: 17%; 7C–13T–5L–5S–3Ca: 14%; 7C–13T–4L–5S–3Ca: 7%). The ancestral hominoid likely had either three (58%) or four (36%) coccygeal vertebrae (95% HPD two to four).

The LCA of hylobatids is firmly resolved as having had 25 presacral vertebrae, including five lumbar vertebrae (>99% for both). The most common single formula is 7C–13T–5L–4S–3Ca (67%). The LCA of hominids is recovered as having 24 presacral vertebrae (75%; 95% HPD 23–25), including four lumbar vertebrae (76%; 95% HPD four to five). The number of precaudal and total vertebrae in the LCA of hominids is more poorly resolved (32 total vertebrae: 47%; 33 total vertebrae: 43%; 29 precaudal: 60%; 30 precaudal: 30%; 95% HPD 28–30), in part due to uncertainty over the number of sacral vertebrae the ancestral hominid had (five [57%] or six [37%] are the most common; 95% HPD four to six). The ancestral hominid is resolved as having three caudal vertebrae (75%; 95% HPD two to four). The most common precise formulae for the LCA of hominids are 7C–13T–4L–5S–3Ca (27%), 7C–13T–4L–6S–3Ca (20%), and 7C–13T–4L–5S–4Ca (10%).

Ancestral hominines are recovered as having 24 presacral vertebrae (83%; 95% HPD 23–24), including four lumbar vertebrae (85%; 95% HPD three to five), likely six (67%) or possibly five (33%) sacral vertebrae (95% HPD five to six), and three (72%; 95% HPD two to four) caudal vertebrae. The most common single formula is

7C–13T–4L–6S–3C (39%). This ancestral hominine pattern is retained in the LCA of chimpanzees and humans, with 24 presacral vertebrae (93%; 95% HPD 23 or 24), four lumbar vertebrae (89%; 95% HPD four or five), six sacral vertebrae (70%; 95% HPD five or six) and three caudal vertebrae (63%; 95% HPD two to four). The most common single formula is 7C–13T–4L–6S–3Ca (43%). No other formulae are above 15%, although 7C–13T–4L–5S–4Ca has 14%, and formulae that are  $\pm$ one caudal vertebra total 59%. Formulae that involve 33 total vertebrae were reconstructed in 64% of simulations. *Gorilla* may have undergone a reduction in the number of both lumbar (three lumbar vertebrae: 63%; four lumbar vertebrae 37%; 95% HPD three to four) and caudal (two caudal vertebrae: 46%; three caudal vertebrae: 46%; 95% HPD two to four) vertebrae. The most common formulae for the ancestor of *Gorilla* are 7C–13T–3L–6S–2Ca (39%) and 7C–13T–4L–6S–3Ca (30%). *Pongo* underwent a reduction in presacral vertebrae (23 presacral vertebrae: >99%). The most common formula for the ancestor of crown *Pongo* is 7C–12T–4L–5S–3Ca (63%), with 7C–12T–4L–6S–3Ca (24%) notable as well.

#### 4. Discussion

We performed two ancestral state reconstructions: analysis 1, which includes a broad sampling of primates and euarchontoglires but excludes caudal vertebrae counts, and analysis 2, which focuses on hominoids and appropriate outgroups and includes caudal vertebral counts. Results of analyses 1 and 2 are broadly similar, but analysis 1 has greater resolution at most nodes. The additional uncertainty in analysis 2 compared with analysis 1 makes sense since analysis 2 includes fewer taxa and more potential variants (inclusion of caudal/coccygeal vertebra number). Despite this, the results of both analyses generally look similar in how they relate to the long-back, intermediate-back, and short-

**Table 3**

Summary of selected results of analysis 2, including full formula and lumbar counts.

Node	Full formulae >5%	Posterior probability (full formula)	Lumbar counts >5%	Posterior probability (lumbar count)	95% highest posterior density for lumbar count
Hominoids	7C 13T 5L 4S 3Ca	18.1%	5	69.4%	4–6
	7C 13T 5L 4S 4Ca	16.9%	4	19.0%	
	7C 13T 5L 5S 3Ca	15.3%	6	11.2%	
	7C 13T 4L 5S 3Ca	7.4%			
Hylobatids	7C 13T 5L 4S 3Ca	67.4%	5	99.7%	5
	7C 13T 5L 4S 2Ca	11.0%			
	7C 13T 5L 5S 3Ca	10.3%			
	7C 13T 5L 5S 2Ca	6.9%			
Hominids	7C 13T 4L 5S 3Ca	26.5%	4	75.7%	4–5
	7C 13T 4L 6S 3Ca	20.9%	5	20.8%	
	7C 13T 4L 5S 4Ca	9.7%			
	7C 13T 5L 5S 3Ca	5.7%			
Hominines	7C 12T 5L 5S 3Ca	5.4%			3–5
	7C 12T 4L 6S 3Ca	5.1%			
	7C 13T 4L 6S 3Ca	39.8%	4	85.0%	
	7C 13T 4L 5S 3Ca	16.7%	3	8.4%	
Pongo	7C 13T 4L 5S 4Ca	9.6%	5	6.6%	4
	7C 13T 4L 6S 2Ca	6.5%			
	7C 13T 3L 6S 3Ca	5.1%			
	7C 12T 4L 5S 3Ca	62.9%	4	99.8%	
Gorilla	7C 12T 4L 6S 3Ca	24.1%			3–4
	7C 12T 4L 6S 2Ca	10.3%			
	7C 13T 3L 6S 2Ca	39.7%	3	63.1%	
	7C 13T 4L 6S 3Ca	29.9%	4	36.9%	
Homo-Pan	7C 13T 3L 6S 3Ca	15.2%			4–5
	7C 13T 3L 6S 4Ca	8.1%			
	7C 13T 4L 6S 3Ca	42.6%	4	89.2%	
	7C 13T 4L 5S 4Ca	14.0%	5	8.9%	
Pan	7C 13T 4L 6S 4Ca	11.5%			4
	7C 13T 4L 5S 3Ca	11.0%			
	7C 13T 4L 6S 2Ca	5.2%			
	7C 13T 4L 6S 3Ca	53.1%	4	98.0%	
	7C 13T 4L 6S 4Ca	21.0%			
	7C 13T 4L 6S 2Ca	11.5%			
	7C 13T 4L 5S 3Ca	6.5%			
	7C 13T 4L 5S 4Ca	5.6%			

Abbreviations: C = cervical vertebrae; T = thoracic vertebrae; L = lumbar vertebrae; S = sacral vertebrae; Ca = caudal (or coccygeal) vertebrae.

back models: Hominoids are found to depart from most other primates (and mammals; Williams et al., 2019b) in reducing their number of presacral vertebrae from 26 to 25, and hominids reduce this further from 25 to 24. The biggest difference between the two analyses is in the number of sacral vertebrae in hominines and the LCA<sub>H-P</sub>. Analysis 1 recovers somewhat stronger support for 5 sacral vertebrae, whereas analysis 2 recovers more substantial support for 6 sacral vertebrae at both nodes. Interestingly, the previous ancestral state reconstruction on vertebral formulae also reported quite a bit of uncertainty regarding the presence of five or six sacral vertebrae at this node, despite utilizing somewhat different methods and incorporating fossil taxa (Thompson and Alméjida, 2017). Given that chimpanzees, bonobos, and western gorillas are all highly polymorphic for these traits, this uncertainty is perhaps unsurprising and may represent real variation in ancestral hominoids.

Overall, our results strongly support the hypothesis that lumbar reduction is a shared derived trait of hominoids (Pilbeam, 2004; Williams, 2012a; Williams and Russo, 2015; Williams and Pilbeam, 2021) and reject the hypothesis that hominoids retained a long lower back throughout much of their evolution (Lovejoy et al., 2009; Lovejoy and McCollum, 2010; McCollum et al., 2010; Machnicki and Reno, 2020). The reduction of lumbar vertebrae to five or fewer early in ape evolution is strongly supported, while the retention of six lumbar vertebrae in ancestral apes receives much weaker support (Tables 2 and 3). Support for lumbar reduction to four or fewer in great apes is also strong, while the retention of six lumbar vertebrae in ancestral great apes or the LCA<sub>H-P</sub> receives

effectively no support. Indeed, in analysis 1, six or more lumbar vertebrae were never recovered at either of these nodes in any of the 5000 simulations we ran (SOM Table S4) and the support was not much better in analysis 2 (SOM Table S11).

The observed reduction of presacral vertebrae at the base of both hominoids and hominids was accomplished through homeotic shifts at the lumbosacral border, and numbers of precaudal vertebrae remain largely consistent (Fig. 3). These results are consistent with the hypothesis that rostral shifts in the Hox11 expression domain may be responsible for these changes (Davis and Capecchi, 1994; Favier et al., 1995; Wahba et al., 2001; Wellik and Capecchi, 2003; McIntyre et al., 2007). This mechanism for shortening the lumbar column is different than that observed in atelids. In atelids, convergent lumbar shortening was accomplished via caudal shift at the thoracolumbar border, and in the case of atelines, meristic loss of a presacral element (Fig. 2).

The most probable scheme we recover for the evolution of the vertebral column in apes (Fig. 3) is that ancestral catarrhines had the formula 7C–13T–6L–3S with a tail, or were perhaps polymorphic for 7C–13T–6L–3S and 7C–12T–7L–3S. Tail loss (reduction and change in morphology from caudal to coccygeal vertebrae; Russo, 2015) probably characterized the ancestor of crown hominoids, a condition likely inherited from stem hominoids such as *Ekembo* and *Nacholapithecus* (Ward et al., 1991; Nakatsukasa et al., 2003, 2004; Russo, 2016). We recover three or four coccygeal vertebrae as the most likely counts for the ancestor of extant apes. In our analysis, ancestral crown apes exhibited a homeotic shift at the lumbar-sacral border to 7C–13T–5L–4S (Fig. 3). This precaudal

pattern was retained in ancestral hylobatids. The lumbar reduction we observe in crown apes is consistent with the previous formal ancestral state reconstruction on this topic (Thompson and Alméjía, 2017). That study did report the strongest support for 12 thoracic vertebrae in ancestral apes, but the authors expressed very little confidence in this result. They considered 12 thoracic vertebrae a likely consequence of limited outgroups and fossil taxa that were dominated by cercopithecoids and hominins, respectively, a conclusion that is consistent with our study, and its larger outgroup sample, reconstructing 13 thoracic vertebrae at this node.

In our study, we find that ancestral great apes further reduced their presacral vertebrae through an additional homeotic shift at the lumbosacral border, changing their formula to 7C–13T–4L–5S. Orangutans reduced their thoracic count through a meristic shift to 7C–12T–4L–5S, and gorillas further reduced their lumbar count through another homeotic shift at the lumbosacral border to 7C–13T–3L–6S. This result contrasts with previous studies that argue for a crown *Gorilla* node with four lumbar vertebrae (Pilbeam, 2004; Williams, 2011, 2012a; Williams and Russo, 2015; Williams et al., 2016, 2019b; Williams and Pilbeam, 2021). However, the other published formal ancestral state reconstruction (Thompson and Alméjía, 2017) found the same result reported here at the gorilla node. We attribute this discrepancy to the high incidence of three lumbar vertebrae in eastern gorillas (*G. beringei*) and the highly polymorphic presence of three and four lumbar vertebrae in western gorillas (*G. gorilla*). Still, our results point to a great deal of uncertainty at the ancestral *Gorilla* node. One possible interpretation of these results is that the LCA of gorillas was polymorphic for three and four lumbar vertebrae, as are modern western gorillas, but a founder effect led to the loss of the four lumbar character states in eastern gorillas (Williams, 2012a). Since ancestral state reconstruction methods (including both the one used here and the one used by Thompson and Alméjía [2017]) typically model polymorphism as uncertainty surrounding a hypothetical ‘true’ character state, such a scenario would be modeled as exactly the result observed here—with high uncertainty at both the root node and one daughter node, and the second daughter node with high certainty. Unfortunately, it is not possible to differentiate such a scenario from actual uncertainty.

#### 4.1. The last common ancestor of *Homo* and *Pan*

LCA<sub>H-P</sub> likely either retained the ancestral hominid formula of 7C–13T–4L–5S or possessed a longer sacrum (7C–13T–4L–6S). The latter count suggests that the LCA<sub>H-P</sub> may have had an additional precaudal vertebra, making it more similar to bonobos than to chimpanzees (McCollum et al., 2010). Given that most extant African apes, particularly chimpanzees, bonobos, and western gorillas, are highly polymorphic for vertebral counts, it is possible that ancestral apes were as well (Pilbeam, 2004; McCollum et al., 2010; Williams et al., 2016). This polymorphism may be due to a relaxation of selection pressures for mobility at the lumbosacral margin (Galis et al., 2014; Shapiro and Kemp, 2019; Williams et al., 2019b) and possibly related to stiffening of the lower back through lumbar entrapment (Lovejoy and McCollum, 2010; McCollum et al., 2010; Machnicki et al., 2016; Williams et al., 2019a). A polymorphic condition of five or six sacral vertebrae in the LCA<sub>H-P</sub> seems likely and would be consistent with our results. This scenario is also consistent with published short-back scenarios (Pilbeam, 2004; Williams, 2012a; Williams and Russo, 2015; Williams et al., 2016, 2019a; Williams and Pilbeam, 2021) but contradicts long-back (Lovejoy et al., 2009; Lovejoy and McCollum, 2010; McCollum et al., 2010, 2010; Machnicki and Reno, 2020) and intermediate-back (Latimer and Ward, 1993; Haeusler et al., 2002; Machnicki et al., 2016; Tardieu and Haeusler, 2019) models.

Of the three scenarios that have been proposed to explain the condition from which hominins evolved, neither the intermediate-back model nor the long-back model is supported by this study, although counts consistent with the intermediate-back model fall within the 95% HPD LCA<sub>H-P</sub> node in analysis 2 and thus cannot be fully rejected here. We counted the minimum number of changes in vertebral numbers (via either homeotic or meristic change) at major nodes (i.e., hominoid, hylobatid, hominid, hominine, hominin, and the ancestral *Pongo*, *Gorilla*, and *Pan* nodes) in each model (note that in the long-back model, proposed parallel changes in *Pan paniscus* and *Pan troglodytes* are not counted here). The long-back models (McCollum et al., 2010; Machnicki et al., 2016; Machnicki and Reno, 2020) require 11–15 or more changes (minima of 11 in McCollum et al., 2010; 15 in Machnicki et al., 2016; 13 in Machnicki and Reno, 2020; see their figures 4, 2, and 6, respectively) and the predicted vertebral formulae fall outside of the 95% HPD range in our study and receive 0% or near 0% posterior probabilities. The intermediate-back models (Latimer and Ward, 1993; Haeusler et al., 2002) require eight or more changes (see figure 9 in Haeusler et al., 2002 and figure 3 in Machnicki et al., 2016) and fare only slightly better in terms of posterior probabilities in our study. The condition of having five lumbar vertebrae, as predicted by the intermediate-back model, does fall within the 95% HPD range for the hominoid and hominid nodes in both analyses, as well as the hominine and LCA<sub>H-P</sub> node in analysis 2, however, so we are unable to fully reject it here.

There are several versions of the short-back model (Pilbeam, 2004; Williams, 2012a; Williams et al., 2016, 2019a; Williams and Pilbeam, 2021), which receive the highest posterior probabilities by far in our analysis. Most short-back models, which propose the presence of 13 thoracic vertebrae and gains to the number of sacral vertebrae via lumbar sacralization (i.e., homeotic shifts at the lumbosacral border; Pilbeam, 2004; Williams, 2011, 2012a; Williams and Russo, 2015; Williams et al., 2016, 2019a; Williams and Pilbeam, 2021) require five changes. Regarding the LCA<sub>H-P</sub>, all short-back models propose either 7C–13T–4L–5S (Williams, 2011, 2012a; Williams and Russo, 2015; Williams et al., 2016) or 7C–13T–4L–6S (Pilbeam, 2004; Williams and Pilbeam, 2021). These receive the highest and second highest support in both of our analyses. Analysis 1 recovers the best support for 7C–13T–4L–5S, while analysis 2 recovers the strongest support for 7C–13T–4L–6S. In analysis 2, we found the strongest support for an LCA<sub>H-P</sub> condition of 7C–13T–4L–6S–3Ca. The second most strongly supported condition was 7C–13T–4L–5S–4Ca, which represents a homeotic variant of the variant with the strongest support. Indeed, we found moderately strong support for an LCA<sub>H-P</sub> with 33 total vertebrae. A modal number of 33 total vertebrae are found in humans, chimpanzees, bonobos, and western gorillas. Although high amounts of variation are seen in specific vertebral numbers within each species, when vertebrae are grouped into combined presacral (C + T + L) and sacrocaudal (S + Ca) numbers, there is much less variation (i.e., there is a great deal of variation in specific vertebral formula, but most individuals have 24 presacral vertebrae and 9 sacrococcygeal vertebrae; Williams and Pilbeam, 2021).

#### 4.2. Ancestral primates

Primates are tentatively reconstructed with 26 presacral and 3 sacral vertebrae, similar to many mammals (Pilbeam, 2004; Narita and Kuratani, 2005; Williams, 2011; Galis et al., 2014; Williams et al., 2019b). There is a large amount of uncertainty regarding specific formulae, however. The formula with the highest posterior probability is 7C–13T–6L–3S, although 7C–13T–6L–4S and 7C–12T–7L–3S also have posterior probabilities above 15%. Many primate taxa are polymorphic for 7C–13T–6L–3S and



7C–12T–7L–3S, which represent homeotic variants of each other: over one-third of the taxa in our data set that have 29 precaudal vertebrae are polymorphic for these two formulae. Given this pattern, it is very possible that ancestral primates were polymorphic for 7C–12T–7L–3S and 7C–13T–6L–3S as well. These results are consistent with previous work by Schultz and Straus (1945), Pilbeam (2004), and Williams (2011). This pattern appears to be retained at the base of haplorhines, anthropoids, platyrrhines, and catarrhines. The relatively high posterior probability for 7C–13T–6L–4S at the base of primates is more surprising since this formula is not particularly common among primates. However, the posterior probability for three sacral vertebrae in ancestral primates (67%) is over twice as high as that for four sacral vertebrae (32%). This fairly high posterior probability of four sacral vertebrae could represent polymorphism or merely uncertainty. Uncertainty in the number of sacral vertebrae at the ancestral primate node is consistent with similar uncertainty seen at the roots of outgroup clades as well as the deep timespan and long branch lengths in that part of the tree.

Our analysis recovers substantial changes in vertebral numbers at the base of strepsirrhines and loriformes. Both lorids and lemuriformes have increased numbers of presacral vertebrae relative to what we recover for the primate LCA, but galagids do not. In fact, the formula we recover for crown galagids is also our reconstructed ancestral primate formula. This means that additional presacral vertebrae must either be convergent in lorids and lemuriformes or that the formula of galagids represents a reversion to the ancestral primate condition. Our results recover the strongest support for the latter scenario. However, our taxon sample was not chosen to address this question. Since lorids are clearly derived in locomotor behavior and related postcranial morphology, including the vertebral column (Shapiro and Simons, 2002), it is possible that galagids, not lorids, represent the primitive loroid (and potentially strepsirrhine) condition. Additional research on the evolution of vertebral numbers focused on strepsirrhines specifically may be useful to help parse this question.

#### 4.3. The fossil record and vertebral evolution

Ancestral state estimations using only extant taxa, as we have performed in this study, frequently fail to capture the full range of variation that existed throughout the evolutionary history of a clade, and the inclusion of fossils can improve on both ancestral character estimates and evolutionary models (Slater et al., 2012; Monson et al., 2022). This lack of fossil data represents a clear limitation of our study. Unfortunately, no fossils are complete enough to allow their inclusion in our analyses. Even the most complete fossil primate ever discovered, *Darwinius masillae*, does not include a complete vertebral column such that the total, precaudal, or presacral numbers of vertebrae are known (Franzen et al., 2009). Additionally, since many primate taxa are polymorphic, a single specimen is insufficient to capture the full range of variation or even the mode of that species' vertebral formula. Furthermore, the phylogenetic placement of many fossil taxa is uncertain, complicating their inclusion.

Thompson and Almécija's (2017) ancestral state reconstruction, however, was able to include limited fossil taxa due to the fact that they looked at vertebral segments independently, and there are several fossils that preserve whole or nearly whole segments of the vertebral column. Their results were broadly similar to ours—most of their analyses supported an LCA<sub>H-P</sub> with four lumbar vertebrae (short-back model), some with five (intermediate-back model), and almost none with six (long-back model). They accounted for uncertainty by running multiple iterations and making different assumptions about each fossil (e.g., the placement of *Oreopithecus* as a

stem or crown hominoid; the presence of five, six, or seven lumbar vertebrae in *Ekembo*; etc.). Despite the inclusion of fossils, however, they consistently found very little, if any support for the long-back model. Even with the most generous assumptions possible about fossil taxa—six lumbar vertebrae in both *Ardipithecus ramidus* (for which only one lumbar vertebra has been published; Simpson et al., 2019) and *Australopithecus*, and six or seven lumbar vertebrae in *Ekembo* and *Nacholapithecus*, support for an LCA<sub>H-P</sub> with six lumbar vertebrae was always less than 50% and usually much lower. And to produce even this modest support, all of these assumptions were required (e.g., when *Ardipithecus* is assumed to have six lumbar vertebrae, but *Australopithecus* is assumed to have five and *Ekembo* and *Nacholapithecus* are assumed to have six, support for the long-back model is still <1%; see Thompson and Almécija [2017] SOM Fig. S60).

In addition to the long-back model requiring multiple improbable assumptions to receive even modest support, Thompson and Almécija's (2017) inclusion of fossils and the resulting increase in uncertainty in phylogenetic relatedness may have represented an additional, inherent bias in favor of the long-back model. Simulations have shown that when there is high uncertainty in phylogenetic trees, ancestral state reconstructions tend to recover more independent origins of traits (Duchêne and Lanfear, 2015). The long-back model requires a shorter back to evolve repeatedly in extant great apes (Fig. 1). Overall, both formal ancestral state reconstruction analyses performed to date have found the strongest support for the short-back model and effectively no support for the long-back model, despite using different approaches—Thompson and Almécija (2017) included fossils but could not include a method that accounted for homeotic changes, while we utilized a method that accounts for both homeotic and meristic change but could not include fossils.

#### 4.4. Comparisons with known fossils

Although we do not include fossils in our study due to their incompleteness, we consider partial fossil vertebral columns here, allowing an independent test of hypotheses generated by our study.

The most complete primate fossil so far discovered, *D. masillae*, includes complete cervical (7C), lumbar (7L), sacral (3S), and caudal (31) regions, but the thoracic column is incomplete, and it is stated that “11 thoracic vertebrae are present although their exact number is difficult to determine and therefore somewhat ambiguous” (Franzen et al., 2009: 12). The phylogenetic position of *Darwinius* is subject to some debate (Franzen et al., 2009; Gingerich et al., 2010; Williams et al., 2010), although a position as a stem strepsirrhine seems likely (Williams et al., 2010). Seven cervical vertebrae, seven lumbar vertebrae, three sacral vertebrae, and greater than 11 thoracic vertebrae in a stem strepsirrhine are consistent with our results.

Other fossil primates are less complete. The stem catarrhine *Epiplioptithecus vindobonensis* is missing vertebrae from both thoracic and lumbar regions (Zapfe, 1958) and, therefore, cannot be used to address issues such as the 12T–7L vs. 13T–6L configuration at the crown catarrhine or haplorhine nodes. Similarly, although numerous Miocene ape partial skeletons are known, only three species preserve more than several vertebrae: *Ekembo nyanzae*, *Nacholapithecus kerioi*, and *Oreopithecus bambolii* (Nakatsukasa, 2019). *Ekembo* and *Nacholapithecus* likely possessed 5–7 lumbar vertebrae and do not preserve complete sacra (Ward, 1993; Nakatsukasa, 2019; Hammond et al., 2020). Given their likely position as stem hominoids (Pugh, 2022), possessing 5–7 lumbar vertebrae is consistent with a reduction from (perhaps polymorphic) six or seven lumbar vertebrae at the crown catarrhine node to five lumbar vertebrae at the crown hominoid node. The



Bac#50 specimen of *Oreopithecus* does preserve a mostly complete sacrum consisting of six elements (but see Haeusler et al., 2002), but it is a different individual from the partial skeleton IGF 11778, which preserves five lumbar vertebrae, and the number of thoracic vertebrae in *Oreopithecus* is unknown (Straus, 1963; Nakatsukasa, 2019; Nakatsukasa, 2019; Hammond et al., 2020). The phylogenetic position of *Oreopithecus* is highly uncertain (Hammond et al., 2020; Pugh, 2022), but five lumbar vertebrae are consistent with a position as a stem hominoid or early-diverging crown hominoid. A six-element sacrum in *Oreopithecus* is more difficult to reconcile with our analyses unless it is a crown hominid, a placement considered highly unlikely (Harrison, 1987; Hammond et al., 2020; Pugh, 2022), but this could also represent one of its many autapomorphies (Delson, 1986). Regardless, a long sacrum is most consistent with the short-back model, consistent with our findings. Unfortunately, potential stem and crown hominids are known from no or too few vertebrae to hypothesize their regional vertebral configurations (Nakatsukasa, 2008, 2019; Nakatsukasa, 2008, 2019; Susanna et al., 2010, 2014).

Fossil hominins are similarly incomplete, with no single skeleton or species known from complete thoracic, lumbar, and sacral regions (Meyer and Williams, 2019; Williams and Meyer, 2019; Machnicki and Reno, 2020), with the exception of Neandertals (Trinkaus, 1983; Arensburg, 1991; Rak, 1991). Regional numbers are known (but sometimes debated) from single individuals in *Australopithecus afarensis* (thoracic and sacral: Russo and Williams, 2015; Machnicki et al., 2016; Williams and Russo, 2016; Ward et al., 2017), *Australopithecus sediba* (lumbar and sacral: Williams et al., 2013, 2018, 2021), *Australopithecus africanus* (lumbar: Haeusler et al., 2002; Rosenman, 2008; Ward et al., 2020), and *Homo erectus* (lumbar and sacral: Haeusler et al., 2002; Schiess and Haeusler, 2013). It has been inferred based on comparative work that *A. ramidus* may have possessed six lumbar vertebrae (Lovejoy et al., 2009; McCollum et al., 2010; but see Williams and Pilbeam, 2021), which would be at odds with our analysis here. Only one lumbar fragment of *A. ramidus* is currently published and was not discovered with the original material at Aramis (Simpson et al., 2019).

Only one Neanderthal preserves a nearly complete precaudal column from which to confidently infer vertebral formula, Kebara 2 (Arensburg, 1991). Kebara 2 may have the same vertebral configuration as modern humans do modally (7C–12T–5L–5S), but the first lumbar vertebra bears riblets ('lumbar ribs') rather than typical costal (lumbar transverse) processes (Ogilvie et al., 1998). Another partial skeleton, Shanidar 3, preserves a few cervical vertebrae and many thoracic vertebrae, along with all elements of the lumbar column and sacrum (Trinkaus, 1983, 1983, 2018; Gómez-Olivencia et al., 2013a; Trinkaus, 2018). Shanidar 3's thoracolumbar transition additionally includes evidence for a caudal shift in vertebral identity: what is frequently referred to as the first lumbar vertebra bears large costal facets on the pedicles (Ogilvie et al., 1998). In both cases (Kebara 2 and Shanidar 3), the criteria established by Schultz and used in this study would identify four lumbar vertebrae and 13 thoracic vertebrae in the case of Kebara 2 (and also likely Shanidar 3). Other nearly complete Neanderthal specimens such as La Chapelle-aux-Saints 1 and Regourdou 1 seem to conform to the modal modern human pattern of 7C–12T–5L (Gómez-Olivencia, 2013; Gómez-Olivencia et al., 2013b), but individual thoracic and lumbar vertebrae are missing, and only the upper sacrum is present in both individuals, precluding assessment of sacral vertebra composition. We did not include Neandertals or other fossil hominins in our analysis for these reasons but note that vertebral counts in these fossils are not inconsistent with the short-back model. This is especially true given the high degree of polymorphism observed in extant hominoid taxa, including humans (which frequently

possess 6S; Williams et al., 2019a). Overall, then, although the lack of fossil data in the ancestral state reconstruction represents a clear limitation of this study, no known fossils contradict our results.

## 5. Conclusions

We performed formal ancestral state reconstructions of the number of vertebrae in primates based on extant taxa and taking into account both homeotic and meristic changes in the vertebral column. We find strong support for the short-back model of ape and human evolution. The long-back model is rejected by our analyses. The intermediate-back model receives little support but cannot be rejected. Our results are necessarily based on extant taxa but are not contradicted by any known fossils. Until potentially contradictory fossil material is discovered, the best-supported hypothesis for the numerical configuration of the vertebral column of the LCA<sub>H-P</sub> is the short-back model. Complete understanding of the contribution of the lower back to positional behavior of the LCA<sub>H-P</sub> requires reconstruction of the location of the transitional vertebra (Shapiro, 1993; Russo, 2010; Williams, 2012b,c; Williams et al., 2013, 2016, 2019a; Williams and Russo, 2015; Thompson and Almécija, 2017; Ward et al., 2017; Nalley et al., 2019; but see Haeusler et al., 2011, 2012), which is beyond the scope of this study. However, a short-backed ancestor is most consistent with great ape-like posture and locomotion; namely, orthograde and probably forelimb-dominated suspensory behaviors in trees and quadrupedal locomotion on the ground (see Williams et al., in press). Future recovery and study of fossil material will test hypotheses on the nature of the LCA<sub>H-P</sub>. Specifically, vertebrae from Miocene and early Pliocene hominins, members of the *Pan* or *Gorilla* lineage, or stem hominines will allow us to more thoroughly test the hypothesis of an African ape-like vertebral formula in the LCA<sub>H-P</sub>.

## Declaration of competing interest

There are no conflicts of interest.

## Acknowledgments

We thank N. Duncan, G. Garcia, E. Hoeger, S. Ketelsen, A. Marcato, B. O'Toole, M. Surovy, and E. Westwig of the American Museum of Natural History; M. Milella, M. Ponce de León, and C. Zollikofer of the Anthropological Institute and Museum, University of Zurich; Y. Haile-Selassie and L. Jellema of Cleveland Museum of Natural History; H. Taboada of the Department of Anthropology, New York University; D. Katz and T. Weaver of the Department of Anthropology, U.C. Davis; B. Patterson, A. Goldman, M. Schulenberg, L. Smith, and W. Stanley of the Field Museum of Natural History; C. McCaffery and D. Reed of Florida Museum of Natural History, University of Florida; J. Chupasko, J. Harrison, and M. Omura of Harvard Museum of Comparative Zoology; E. Gilissen and W. Wendelen of Musée Royal de l'Afrique Centrale; S. Jancke, N. Lange, and F. Mayer of Musée für Naturkunde, Berlin; C. Conroy of the Museum of Vertebrate Zoology, U.C. Berkeley; N. Edminion, L. Gordon, K. Helgen, E. Langan, D. Lunde, J. Ososky, and R. Thorington of the National Museum of Natural History, Smithsonian Institution; J. Soderberg and M. Tappen of Neil C. Tappen Collection, University of Minnesota; S. Bruaux and G. Lenglet of Royal Belgian Institute of Natural Sciences; M. Hiermeier of Zoologische Staatssammlung München; B. Wilkey and I. Livne of Powell-Cotton Museum, Birchingdon; C. Lefèvre of Muséum national d'Histoire naturelle; Paris; D. Grimaud-Hervé, A. Fort, V. Laborde, and L. Huet of Muséum de l'Homme, Paris; R. Portela of the Natural History Museum, London; J. Stock and M. Mirazón Lahr of Duckworth Collection,

University of Cambridge; A. Rodríguez-Hidalgo of Institut Català de Paleoeologia Humana i Evolució Social, Tarragona; the Grant Museum of Zoology, University College of London; and the Oxford University Museum of Natural History for facilitating access to specimens in their care. We thank S. McFarlin for granting us access to images of mountain gorilla specimens, and we are grateful to the Rwandan government for permission to study Virunga mountain gorilla skeletal specimens from the Volcanoes National Park curated by the Mountain Gorilla Skeletal Project, established through the continuous efforts of researchers and staff of the Rwanda Development Board's Department of Tourism and Conservation, Dian Fossey Gorilla Fund, Gorilla Doctors, Institute of National Museums of Rwanda, The George Washington University, and New York University College of Dentistry and funding by the National Science Foundation (BCS-0852866, BCS-0964944, BCS-1520221), National Geographic Society's Committee for Research and Exploration (8486-08), and The Leakey Foundation. J.K.S. was funded through the National Science Foundation (BCS-2041700), the Leakey Foundation, and Sigma Xi. S.A.W. was funded through the National Science Foundation (BCS-0925734), the Leakey Foundation, and the New York University Research Challenge Fund. A.G.-O. was funded by two Synthesys grants (GB-TAF-3674, BE-TAF-4132) and a Marie Curie fellowship (MC-IEF 327243) funded by the European commission, a Ramón y Cajal fellowship by the Ministerio de Ciencia, Innovación y Universidades (RYC-2017-22558), the Grupo IT1485-22 from the Gobierno Vasco/Eusko Jaurlaritza, and the Ministerio de Ciencia e Innovación (project PID2021-122355NB-C31).

## Appendix A. Supplementary Online Material

Supplementary online material to this article can be found online at <https://doi.org/10.1016/j.jhevol.2023.103359>.

## References

- Arensburg, B., 1991. The vertebral column, thoracic cage and hyoid bone. In: Bar-Yosef, O. (Ed.), *Le Squelette Moustérien de Kébara*. Editions du CNRS, Paris, pp. 113–147.
- Arnold, C., Matthews, L.J., Nunn, C.L., 2010. The 10kTrees website: A new online resource for primate phylogeny. *Evol. Anthropol.* 19, 114–118.
- Bininda-Emonds, O.R.P., Cardillo, M., Jones, K.E., MacPhee, R.D.E., Beck, R.M.D., Grenyer, R., Price, S.A., Vos, R.A., Gittleman, J.L., Purvis, A., 2007. The delayed rise of present-day mammals. *Nature* 446, 507–512.
- Bollback, J.P., 2006. SIMMAP: Stochastic character mapping of discrete traits on phylogenies. *BMC Bioinform.* 7, 88.
- Carapuço, M., Nóvoa, A., Bobola, N., Mallo, M., 2005. Hox genes specify vertebral types in the presomitic mesoderm. *Genes Dev.* 19, 2116–2121.
- Casaca, A., Santos, A.C., Mallo, M., 2014. Controlling Hox gene expression and activity to build the vertebrate axial skeleton. *Dev. Dyn.* 243, 24–36.
- Clausier, D.A., 1980. Functional and comparative anatomy of the primate spinal column: Some locomotor and postural adaptations. Ph.D. Dissertation, University of Wisconsin–Milwaukee.
- Davis, A.P., Capecchi, M.R., 1994. Axial homeosis and appendicular skeleton defects in mice with a targeted disruption of *hoxd-11*. *Development* 120, 2187–2198.
- Delson, E., 1986. An anthropoid enigma: Historical introduction to the study of *Oreopithecus bambolii*. *J. Hum. Evol.* 15, 523–531.
- Duchêne, S., Lanfear, R., 2015. Phylogenetic uncertainty can bias the number of evolutionary transitions estimated from ancestral state reconstruction methods. *J. Exp. Zool. B Mol. Dev. Evol.* 324, 517–524.
- Favier, B., Le Meur, M., Chambon, P., Dollé, P., 1995. Axial skeleton homeosis and forelimb malformations in *Hoxd-11* mutant mice. *Proc. Natl. Acad. Sci. USA* 92, 310–314.
- Franzen, J.L., Gingerich, P.D., Habersetzer, J., Hurum, J.H., Koenigswald, W. von, Smith, B.H., 2009. Complete primate skeleton from the Middle Eocene of Messel in Germany: Morphology and paleobiology. *PLoS One* 4, e5723.
- Fulwood, E.L., O'Meara, B.C., 2014. A phylogenetic approach to the evolution of anthropoid lumbar number. *Am. J. Phys. Anthropol.* 153, 123–123.
- Galis, F., 1999a. Why do almost all mammals have seven cervical vertebrae? Developmental constraints, Hox genes, and cancer. *J. Exp. Zool.* 285, 19–26.
- Galis, F., 1999b. On the homology of structures and Hox genes: The vertebral column. In: Bock, G., Cardew, G. (Eds.), *Novartis Foundation Symposium 222 – Homology*. John Wiley & Sons, Ltd, Chichester, pp. 80–94.
- Galis, F., Carrier, D.R., van Alphen, J., van der Mije, S.D., van Dooren, T.J.M., Metz, J.A.J., ten Broek, C.M.A., 2014. Fast running restricts evolutionary change of the vertebral column in mammals. *Proc. Natl. Acad. Sci. USA* 111, 11401–11406.
- Gingerich, P.D., Franzen, J.L., Habersetzer, J., Hurum, J.H., Smith, B.H., 2010. *Darwinius masillae* is a Haplorhine — reply to Williams et al. (2010). *J. Hum. Evol.* 59, 574–579.
- Gómez-Olivencia, A., 2013. Back to the old man's back: Reassessment of the anatomical determination of the vertebrae of the Neandertal individual of La Chapelle-aux-Saints. *Ann. Paleontol.* 99, 43–65.
- Gómez-Olivencia, A., Been, E., Arsuaga, J.L., Stock, J.T., 2013a. The Neandertal vertebral column 1: The cervical spine. *J. Hum. Evol.* 64, 608–630.
- Gómez-Olivencia, A., Couture-Veschambre, C., Madeline, S., Maureille, B., 2013b. The vertebral column of the Regourdou 1 Neandertal. *J. Hum. Evol.* 64, 582–607.
- Haeusler, M., Martelli, S.A., Boeni, T., 2002. Vertebrae numbers of the early hominid lumbar spine. *J. Hum. Evol.* 43, 621–643.
- Haeusler, M., Schiess, R., Boeni, T., 2011. New vertebral and rib material point to modern bauplan of the Nariokotome *Homo erectus* skeleton. *J. Hum. Evol.* 61, 575–582.
- Haeusler, M., Schiess, R., Böni, T., 2012. Modern or distinct axial bauplan in early hominins? A reply to Williams (2012). *J. Hum. Evol.* 63, 557–559.
- Hammond, A.S., Rook, L., Anaya, A.D., Cioppi, E., Costeur, L., Moyà-Solà, S., Almécija, S., 2020. Insights into the lower torso in late Miocene hominoid *Oreopithecus bambolii*. *Proc. Natl. Acad. Sci. USA* 117, 278–284.
- Harrison, T., 1987. A reassessment of the phylogenetic relationships of *Oreopithecus bambolii* Gervais. *J. Hum. Evol.* 15, 541–583.
- Johanson, D.C., Lovejoy, C.O., Kimbel, W.H., White, T.D., Ward, S.C., Bush, M.E., Latimer, B.M., Coppens, Y., 1982. Morphology of the Pliocene partial hominid skeleton (A.L. 288-1) from the Hadar formation, Ethiopia. *Am. J. Phys. Anthropol.* 57, 403–451.
- Latimer, B.M., Ward, C.V., 1993. The thoracic and lumbar vertebrae. In: Walker, A.C., Leakey, R. (Eds.), *The Nariokotome Homo Erectus*. Harvard University Press, Cambridge, pp. 266–293.
- Lewis, P.O., 2001. A likelihood approach to estimating phylogeny from discrete morphological character data. *Syst. Biol.* 50, 913–925.
- Lovejoy, C.O., 2005. The natural history of human gait and posture: Part 2. Hip and thigh. *Gait Posture* 21, 113–124.
- Lovejoy, C.O., McCollum, M.A., 2010. Spinopelvic pathways to bipedality: Why no hominids ever relied on a bent-hip–bent-knee gait. *Philos. Trans. R. Soc. B Biol. Sci.* 365, 3289–3299.
- Lovejoy, C.O., Suwa, G., Simpson, S.W., Matternes, J.H., White, T.D., 2009. The great divides: *Ardipithecus ramidus* reveals the postcrania of our last common ancestors with African apes. *Science* 326, 73–106.
- MacArthur, R.H., 1957. On the relative abundance of bird species. *Proc. Natl. Acad. Sci. USA* 43, 293–295.
- Machnicki, A.L., Reno, P.L., 2020. Great apes and humans evolved from a long-backed ancestor. *J. Hum. Evol.* 144, 102791.
- Machnicki, A.L., Lovejoy, C.O., Reno, P.L., 2016. Developmental identity versus typology: Lucy has only four sacral segments. *Am. J. Phys. Anthropol.* 160, 729–739.
- Mallo, M., Wellik, D.M., Deschamps, J., 2010. Hox genes and regional patterning of the vertebrate body plan. *Dev. Biol.* 344, 7–15.
- McCollum, M.A., Rosenman, B.A., Suwa, G., Meindl, R.S., Lovejoy, C.O., 2010. The vertebral formula of the last common ancestor of African apes and humans. *J. Exp. Zool. B Mol. Dev. Evol.* 314B, 123–134.
- McIntyre, D.C., Rakshit, S., Yallowitz, A.R., Loken, L., Jeannotte, L., Capecchi, M.R., Wellik, D.M., 2007. Hox patterning of the vertebrate rib cage. *Development* 134, 2981–2989.
- Meyer, M.R., Williams, S.A., 2019. The spine of Early Pleistocene *Homo*. In: Been, E., Gómez-Olivencia, A., Ann Kramer, P. (Eds.), *Spinal Evolution: Morphology, Function, and Pathology of the Spine in Hominoid Evolution*. Springer International Publishing, Cham, pp. 153–183.
- Monson, T.A., Brasil, M.F., Mahaney, M.C., Schmitt, C.A., Taylor, C.E., Hlusko, L.J., 2022. Keeping 21st century paleontology grounded: Quantitative genetic analyses and ancestral state reconstruction re-emphasize the essentiality of fossils. *Biology* 11, 1218.
- Nakatsukasa, M., 2008. Comparative study of Moroto vertebral specimens. *J. Hum. Evol.* 55, 581–588.
- Nakatsukasa, M., 2019. Miocene ape spinal morphology: The evolution of orthograde. In: Been, E., Gómez-Olivencia, A., Ann Kramer, P. (Eds.), *Spinal Evolution: Morphology, Function, and Pathology of the Spine in Hominoid Evolution*. Springer International Publishing, Cham, pp. 73–96.
- Nakatsukasa, M., Tsujikawa, H., Shimizu, D., Takano, T., Kunitatsu, Y., Nakano, Y., Ishida, H., 2003. Definitive evidence for tail loss in *Nacholapithecus*, an East African Miocene hominoid. *J. Hum. Evol.* 45, 179–186.
- Nakatsukasa, M., Ward, C.V., Walker, A., Teaford, M.F., Kunitatsu, Y., Ogihara, N., 2004. Tail loss in *Proconsul heseloni*. *J. Hum. Evol.* 46, 777–784.
- Nalley, T.K., Scott, J.E., Ward, C.V., Alemseged, Z., 2019. Comparative morphology and ontogeny of the thoracolumbar transition in great apes, humans, and fossil hominins. *J. Hum. Evol.* 134, 102632.
- Narita, Y., Kuratani, S., 2005. Evolution of the vertebral formulae in mammals: A perspective on developmental constraints. *J. Exp. Zool. B Mol. Dev. Evol.* 304B, 91–106.
- Ogilvie, M.D., Hilton, C.E., Ogilvie, C.D., 1998. Lumbar anomalies in the Shanidar 3 Neandertal. *J. Hum. Evol.* 35, 597–610.

- Pilbeam, D., 2004. The anthropoid postcranial axial skeleton: Comments on development, variation, and evolution. *J. Exp. Zool. B Mol. Dev. Evol.* 302B, 241–267.
- Plummer, M., Best, N., Cowles, K., Vines, K., 2006. CODA: Convergence diagnosis and output analysis for MCMC. *R. News* 6, 7–11.
- Pugh, K.D., 2022. Phylogenetic analysis of Middle-Late Miocene apes. *J. Hum. Evol.* 165, 103140.
- R Core Team, 2022. R: A language and environment for statistical computing. R foundation for statistical computing, Vienna.
- Rak, Y., 1991. The pelvis. In: Bar-Yosef, O. (Ed.), *Le Squelette Moustérien de Kébara*. Editions du CNRS, Paris, pp. 147–156.
- Revell, L.J., 2012. phytools: An R package for phylogenetic comparative biology (and other things). *Methods Ecol. Evol.* 3, 217–223.
- Rosenman, B., 2008. Triangulating the evolution of the vertebral column in the last common ancestor: Thoracolumbar transverse process homology in the Hominoidea. Ph.D. Dissertation, Kent State University.
- Russo, G.A., 2010. Prezygapophyseal articular facet shape in the catarrhine thoracolumbar vertebral column. *Am. J. Phys. Anthropol.* 142, 600–612.
- Russo, G.A., 2015. Postsacral vertebral morphology in relation to tail length among primates and other mammals. *Anat. Rec.* 298, 354–375.
- Russo, G.A., 2016. Comparative sacral morphology and the reconstructed tail lengths of five extinct primates: *Proconsul heseloni*, *Epipliothecus vindobonensis*, *Archaeolemur edwardsi*, *Megaladapis grandidieri*, and *Palaeopropithecus kelyus*. *J. Hum. Evol.* 90, 135–162.
- Russo, G.A., Williams, S.A., 2015. “Lucy” (A.L. 288-1) had five sacral vertebrae. *Am. J. Phys. Anthropol.* 156, 295–303.
- Schiess, R., Haeusler, M., 2013. No skeletal dysplasia in the Nariokotome boy KNM-WT 15000 (*Homo erectus*)—A reassessment of congenital pathologies of the vertebral column. *Am. J. Phys. Anthropol.* 150, 365–374.
- Schultz, A.H., 1950. The physical distinctions of man. *Proc. Am. Philos. Soc.* 94, 428–449.
- Schultz, A.H., 1961. Vertebral column and thorax. *Primates* 4, 1–66.
- Schultz, A.H., Straus, W.L., 1945. The numbers of vertebrae in primates. *Proc. Am. Philos. Soc.* 89, 601–626.
- Shapiro, L., 1993. Functional morphology of the vertebral column in primates. In: Gebo, D.L. (Ed.), *Postcranial Adaptation in Nonhuman Primates*. Northern Illinois University Press, Dekalb, pp. 121–149.
- Shapiro, L.J., Kemp, A.D., 2019. Functional and developmental influences on intraspecific variation in catarrhine vertebrae. *Am. J. Phys. Anthropol.* 168, 131–144.
- Shapiro, L.J., Simons, C.V.M., 2002. Functional aspects of strepsirrhine lumbar vertebral bodies and spinous processes. *J. Hum. Evol.* 42, 753–783.
- Simpson, S.W., Levin, N.E., Quade, J., Rogers, M.J., Semaw, S., 2019. *Ardipithecus ramidus* postcrania from the Gona project area, Afar Regional State, Ethiopia. *J. Hum. Evol.* 129, 1–45.
- Slater, G.J., Harmon, L.J., Alfaro, M.E., 2012. Integrating fossils with molecular phylogenies improves inference of trait evolution: Fossils, phylogenies, and models of trait evolution. *Evolution* 66, 3931–3944.
- Springer, M.S., Meredith, R.W., Gatesy, J., Emerling, C.A., Park, J., Rabosky, D.L., Stadler, T., Steiner, C., Ryder, O.A., Janečka, J.E., Fisher, C.A., Murphy, W.J., 2012. Macroevolutionary dynamics and historical biogeography of primate diversification inferred from a species supermatrix. *PLoS One* 7, e49521.
- Straus, W.L., 1963. The classification of *Oreopithecus*. In: Washburn, S.L. (Ed.), *Classification and Human Evolution*. Routledge, London, pp. 146–177.
- Susanna, I., Alba, D.M., Almécija, S., 2010. Las vertebrae lumbares del gran simio antropomorfo basal del Mioceno Medio *Pierolapithecus catalaunicus* (Primates: Hominoidea). *Cidaris* 30, 311–316.
- Susanna, I., Alba, D.M., Almécija, S., Moyà-Solà, S., 2014. The vertebral remains of the late Miocene great ape *Hispanopithecus laietanus* from Can Llobateres 2 (Vallès-Penedès Basin, NE Iberian Peninsula). *J. Hum. Evol.* 73, 15–34.
- Tague, R.G., 2017. Sacral variability in tailless species: *Homo sapiens* and *Ochotona princeps*. *Anat. Rec.* 300, 798–809.
- Tardieu, C., Haeusler, M., 2019. The acquisition of human verticality with an emphasis on sagittal balance. In: Roussouly, P., Pinheiro-Franco, J.L., Labelle, H., Gehrechen, M. (Eds.), *Sagittal Balance of the Spine*. Thieme Publishers, New York, pp. 13–22.
- Thompson, N.E., Almécija, S., 2017. The evolution of vertebral formulae in Hominoidea. *J. Hum. Evol.* 110, 18–36.
- Trinkaus, E., 1983. *The Shanidar Neandertals*. Academic Press, Cambridge.
- Trinkaus, E., 2018. An abundance of developmental anomalies and abnormalities in Pleistocene people. *Proc. Natl. Acad. Sci. USA* 115, 11941–11946.
- Upham, N.S., Esselstyn, J.A., Jetz, W., 2019. Inferring the mammal tree: Species-level sets of phylogenies for questions in ecology, evolution, and conservation. *PLoS Biol.* 17, e3000494.
- Wahba, G.M., Hostikka, S.L., Carpenter, E.M., 2001. The paralogous Hox genes Hoxa10 and Hoxd10 interact to pattern the mouse hindlimb peripheral nervous system and skeleton. *Dev. Biol.* 231, 87–102.
- Ward, C.V., 1993. Torso morphology and locomotion in *Proconsul nyanzae*. *Am. J. Phys. Anthropol.* 92, 291–328.
- Ward, C.V., Walker, A., Teaford, M.F., 1991. *Proconsul* did not have a tail. *J. Hum. Evol.* 21, 215–220.
- Ward, C.V., Nalley, T.K., Spoor, F., Tafforeau, P., Alemseged, Z., 2017. Thoracic vertebral count and thoracolumbar transition in *Australopithecus afarensis*. *Proc. Natl. Acad. Sci. USA* 114, 6000–6004.
- Ward, C.V., Rosenman, B., Latimer, B.M., Nalla, S., 2020. Thoracolumbar vertebrae and ribs. In: Zipfel, B., Richmond, B.G., Ward, C.V. (Eds.), *Hominin Postcranial Remains from Sterkfontein, South Africa, 1936–1995*. Oxford University Press, Oxford, pp. 144–186.
- Wellik, D.M., Capecchi, M.R., 2003. Hox10 and Hox11 genes are required to globally pattern the mammalian skeleton. *Science* 301, 363–367.
- Whitcome, K.K., Shapiro, L.J., Lieberman, D.E., 2007. Fetal load and the evolution of lumbar lordosis in bipedal hominins. *Nature* 450, 1075–1078.
- Williams, B.A., Kay, R.F., Kirk, E.C., Ross, C.F., 2010. *Darwinius masillae* is a strepsirrhine—A reply to Franzen et al. (2009). *J. Hum. Evol.* 59, 567–573.
- Williams, S.A., 2011. Evolution of the hominoid vertebral column. Ph.D. Dissertation, University of Illinois at Urbana-Champaign.
- Williams, S.A., 2012a. Variation in anthropoid vertebral formulae: Implications for homology and homoplasy in hominoid evolution. *J. Exp. Zool. B Mol. Dev. Evol.* 318, 134–147.
- Williams, S.A., 2012b. Placement of the diaphragmatic vertebra in catarrhines: Implications for the evolution of dorsostability in hominoids and bipedalism in hominins. *Am. J. Phys. Anthropol.* 148, 111–122.
- Williams, S.A., 2012c. Modern or distinct axial bauplan in early hominins? Comments on Haeusler et al. (2011). *J. Hum. Evol.* 63, 552–556.
- Williams, S.A., Meyer, M.R., 2019. The spine of *Australopithecus*. In: Been, E., Gómez-Olivencia, A., Ann Kramer, P. (Eds.), *Spinal Evolution: Morphology, Function, and Pathology of the Spine in Hominoid Evolution*. Springer International Publishing, Cham, pp. 125–151.
- Williams, S.A., Pilbeam, D., 2021. Homeotic change in segment identity derives the human vertebral formula from a chimpanzee-like one. *Am. J. Phys. Anthropol.* 176, 283–294.
- Williams, S.A., Russo, G.A., 2015. Evolution of the hominoid vertebral column: The long and the short of it. *Evol. Anthropol.* 24, 15–32.
- Williams, S.A., Russo, G.A., 2016. The fifth element (of Lucy's sacrum): Reply to Machnicki, Lovejoy, and Reno. *Am. J. Phys. Anthropol.* 161, 374–378.
- Williams, S.A., Ostrofsky, K.R., Frater, N., Churchill, S.E., Schmid, P., Berger, L.R., 2013. The vertebral column of *Australopithecus sediba*. *Science* 340, 1232996.
- Williams, S.A., Middleton, E.R., Villamil, C.I., Shattuck, M.R., 2016. Vertebral numbers and human evolution. *Am. J. Phys. Anthropol.* 159, 19–36.
- Williams, S.A., Meyer, M.R., Nalla, S., García-Martínez, D., Nalley, T.K., Eyre, J., Prang, T.C., Bastir, M., Schmid, P., Churchill, S.E., 2018. The vertebrae, ribs, and sternum of *Australopithecus sediba*. *PaleoAnthropology* 2018, 156–233.
- Williams, S.A., Gómez-Olivencia, A., Pilbeam, D.R., 2019a. Numbers of vertebrae in hominoid evolution. In: Been, E., Gómez-Olivencia, A., Ann Kramer, P. (Eds.), *Spinal Evolution: Morphology, Function, and Pathology of the Spine in Hominoid Evolution*. Springer International Publishing, Cham, pp. 97–124.
- Williams, S.A., Spear, J.K., Petrucci, L., Goldstein, D.M., Lee, A.B., Peterson, A.L., Miano, D.A., Kaczmarek, E.B., Shattuck, M.R., 2019b. Increased variation in numbers of presacral vertebrae in suspensory mammals. *Nat. Ecol. Evol.* 3, 949–956.
- Williams, S.A., Prang, T.C., Meyer, M.R., Nalley, T.K., Van Der Merwe, R., Yelverton, C., García-Martínez, D., Russo, G.A., Ostrofsky, K.R., Spear, J., Eyre, J., Grabowski, M., Nalla, S., Bastir, M., Schmid, P., Churchill, S.E., Berger, L.R., 2021. New fossils of *Australopithecus sediba* reveal a nearly complete lower back. *eLife* 10, e70447.
- Williams, S.A., Zeng, I., Paton, G.J., Yelverton, C., Dunham, C., Ostrofsky, K.R., Shukman, S., Avilez, M.V., Eyre, J., Loewen, T., Prang, T.C., Meyer, M.R., 2022. Inferring lumbar lordosis in Neandertals and other hominins. *Proc. Natl. Acad. Sci. Nexus* 1, pgab005.
- Williams, S.A., Prang, T.C., Russo, G.A., Young, N.M., Gebo, D.L., in press. African apes and the evolutionary history of orthograde and bipedalism. *Yearb. Biol. Anthropol. Biol. Anthropol.* <https://doi.org/10.1002/ajpa.24684>
- Zapfe, H., 1958. The skeleton of *Pliopithecus (Epipliothecus) vindobonensis* Zapfe and Hürzeler. *Am. J. Phys. Anthropol.* 16, 441–457.